8-1980

Removal of Sulfur Dioxide and Nitric Oxide From a Flue Gas Stream By Two Sodium Alkalis of Various Sizes

John R. Carson
University of Tennessee - Knoxville

To the Graduate Council:

I am submitting herewith a thesis written by John R. Carson entitled "Removal of Sulfur Dioxide and Nitric Oxide From a Flue Gas Stream By Two Sodium Alkalis of Various Sizes." I have examined the final electronic copy of this thesis for form and content and recommend that it be accepted in partial fulfillment of the requirements for the degree of Master of Science, with a major in Environmental Engineering.

Wayne T. Davis, Major Professor

We have read this thesis and recommend its acceptance:

ARRAY(0x7f702f8fc2d8)

Accepted for the Council:
Dixie L. Thompson

Vice Provost and Dean of the Graduate School

(Original signatures are on file with official student records.)

To the Graduate Council:

I am submitting herewith a thesis written by John R. Carson Entitled "Removal of Sulfur Dioxide and Nitric Oxide From a Flue Gas Stream By Two Sodium Alkalis of Various Sizes." I recommend that it be accepted in partial fulfillment of the requirements for the degree of Master of Science, with a major in Environmental Engineering.

Wayne T. Davis

Wayne T. Davis, Major Professor

We have read this thesis
and recommend its acceptance:

Daniel W. West

Roger C. Memon

Accepted for the Council:

L. Evans Reed

Vice Chancellor
Graduate Studies and Research

REMOVAL OF SULFUR DIOXIDE AND NITRIC OXIDE FROM A FLUE GAS STREAM BY TWO SODIUM ALKALIS OF VARIOUS SIZES

A Thesis

Presented for the

Master of Science

Degree

The University of Tennessee, Knoxville

John R. Carson

August 1980

ACKNOWLEDGEMENTS

This research was conducted at the University of Tennessee in Knoxville and was partially sponsored by the Pollution Control Division of Carborundum Environmental Systems, Inc. The sodium bicarbonate used in the study was donated by the Church and Dwight Company.

The author is indebted to Dr. Wayne T. Davis, his major professor, for the encouragement and constructive criticism that he has provided throughout their association.

Appreciation is also extended to Carolyn Carson for typing the rough draft and for being a sympathetic, understanding wife during the author's graduate study.

Special thanks are also expressed to Bill Long, Jim Frei, Sherman Green, Jeff McIntosh, and Gail Ferguson.

ABSTRACT

The primary purpose of this research effort was to examine the dry removal of SO_2 and NO from a flue gas stream by injecting two sodium additives into a pilot bag house system. The additives tested were $NaHCO_3$ and Na_2CO_3 dusts with mass mean diameters ranging from approximately 30 to 200 microns. The Na_2CO_3 was obtained by decomposing the $NaHCO_3$ (with heat) prior to testing. The bag house temperature was maintained at either 250 or 300 degrees F.

It was demonstrated that 70% SO_2 removal can be attained with $NaHCO_3$ powders that have mass mean diameters of 32 and 52 microns at stoichiometric ratios of 0.8 and 1.3, respectively. The rate of mass transfer limited the desulfurization capacity of $NaHCO_3$ powders with mass mean diameters greater than 50 microns. The rate of chemical reaction limited the SO_2 removal capability of the smallest $NaHCO_3$ additive tested (mass mean diameter=32 microns). Decomposition of $NaHCO_3$ to Na_2CO_3 in bulk before injection yielded poorer SO_2 removal.

It was also demonstrated that 7 to 36 % of the NO was removed simultaneously with SO_2 by the $NaHCO_3$ additives with mass mean diameters smaller than 120 microns. This removal was inversely dependent on the system temperature. No appreciable NO removal was observed with Na_2CO_3 injection.

TABLE OF CONTENTS

LIST OF TABLES

LIST OF FIGURES

INTRODUCTION

The discharge of pollutants into the atmosphere by steam electric generating plants accounts for appreciable amounts of national emissions. For example, in 1976 24% of the particulate, 65% of the sulfur dioxide (SO_2), and 29% of the nitrous oxides (NO_x) were attributed to these sources. In addition, a 50% increase in the number of fossil-fuel-fired utility plants is planned within the next 10 years. Coal consumption alone will increase from 400 million tons/year in 1975 to 1250 million tons/year in 1995 (1). Passage of the Clean Air Act (1970), New Source Performance Standards (1971), and subsequent legislation has required that these pollutants emitted by fossil-fuel-fired utility boilers be controlled. The emission standards for total particulate, sulfur dioxide (SO_2) and the oxides of nitrogen (NO_x) are specified in Table 1. Particulate control can be accomplished with electrostatic precipitators or fabric filters (bag houses). The electric power industry is required to apply the "best demonstrated technology" for SO_2 and NO_x control (1). NO_x emissions can probably be best controlled by combustion modification. The reduction of SO_2 emissions requires one or more of the following removal techniques: precleaning of the fuel, removal of sulfur containing material during combustion, and wet or dry scrubbing of the flue gas stream.

Table 1. Federal Standards of Performance for New Electric Utility Steam Generating Units (>73 MW with heat input >250 million BTU/hr [reference 1]).

Pollutant	Standard
Particulate	0.03 lb/million BTU
SO_2	1.20 lb/million BTU and 90% reduction or (when <0.60 lb/million BTU) 70% reduction
NO_x (Anthracite, Bituminous and Lignite)	0.60 lb/million BTU
NO_x (Subbituminous)	0.50 lb/million BTU

One method of dry scrubbing involves the injection of nahcolite into either the combustion chamber or the flue gas ductwork of a fossil-fuel-fired boiler. Nahcolite is a naturally occurring ore that is approximately 70% sodium bicarbonate ($NaHCO_3$). The solid nahcolite reacts with the gaseous SO_2 and is collected along with the flyash in a particulate control device. The most effective utilization of this technique occurs when a bag house collector is used to clean the particulate laden exhaust stream. The dust cake on the filtration surface provides an additional site for reaction of the SO_2 with the ore.

The primary purpose of this research effort was to examine certain facets of this gas/solid removal technique using a 1000 acfm fabric filter system. The specific objectives were:

a. Evaluate the removal of SO_2 by $NaHCO_3$ dusts of five different mass mean diameters (MMD). The mass mean diameters of these dusts ranged from approximately 30 to 200 microns.

b. Convert these five dusts to a more porous form (Na_2CO_3) by heating and compare their SO_2 removal capabilities with those of raw $NaHCO_3$.

c. Determine whether $NaHCO_3$ or the Na_2CO_3 can be utilized for NO removal in such a system.

I. LITERATURE REVIEW

The use of fabric filters (bag houses) for particulate control of effluent gases is a common practice. This method of pollution control has gained increased acceptance by that portion of the electric utility industry that relies on fossil fuels for combustion energy. This is due primarily to the enactment of more stringent emission requirements. Although fabric filtration systems (bag houses) have traditionally been installed for particulate control, such a system can also be employed to remove sulfur dioxide (SO_2). This can be accomplished by injecting some reactive material either into the boiler system upstream of the bag house, directly into the bag house, or by a combination of these techniques. The fabric filter then functions as both a particulate control device and a chemical contacting device.

Several compounds have been evaluated for this use. Liu and Chaffee (2) conducted such tests on a pilot bag house at Mercer Generating Station (New Jersey) in 1969. The additives tested were sodium bicarbonate, nahcolite, and lime. The best SO_2 removal with hydrated lime was 49%. This occurred at a temperature of 640 degrees F and a stoichiometric ratio of 3.0. The stoichiometric ratio relates the actual molar additive injection rate to the

theoretical rate required to react with the SO_2 in the system. Thus, a stoichiometric ratio of 3.0 means that 300% of the additive theoretically required to react with the SO_2 was actually injected. Sodium bicarbonate ($NaHCO_3$) injection produced significantly higher removal efficiencies at lower temperatures and injection rates. For example, $NaHCO_3$ injection at a stoichiometric ratio of 1.0 at 530 degrees F affected a SO_2 removal efficiency of 86%. Veazie and Kielmeyer (3) tested seven materials as SO_2 sorbents in a bag house at temperatures ranging from 300-1000 degrees F. The materials tested were four slaked limes, manganese dioxide, alkalized alumina, and nahcolite. Of these materials only the alumina and the nahcolite were effective in removing SO_2 at temperatures within the range of typical bag house operation (300-500 degrees F). Bechtel Corporation (4), in a 1976 report to EPRI, concluded that of the various agents evaluated for SO_2 removal in bag house systems (limestones, dolomites, quicklime, hydrated lime, manganese dioxide, sodium bicarbonate, sodium carbonate, and potassium permanganate), only sodium carbonate and sodium bicarbonate were effective SO_2 removal compounds. Hartman (5) reiterated these conclusions after comparing decomposed $NaHCO_3$, magnesium oxide (MgO), and calcined limestone (CaO) as SO_2 removal agents in a fixed bed reactor. The rate at which the decomposed $NaHCO_3$ at 300

degrees F reacted with SO_2 was higher by more than an order of magnitude than that of MgO at 1380 degrees F or CaO at 1560 degrees F.

Nahcolite

Nahcolite is a naturally occurring ore that is approximately 70% sodium bicarbonate ($NaHCO_3$). It is present in vast quantities in the oil shales of the Green River formation in northwestern Colorado, northeast Utah, and southwest Wyoming. The total mineral present is about 29 billion tons (6). This area would probably supply nahcolite for full scale sulfur dioxide removal enterprises. Nahcolite (sodium bicarbonate) decomposes without melting into soda ash (sodium carbonate), water, and carbon dioxide according to the following equation:

$$2NaHCO_3 \rightleftharpoons Na_2CO_3 + H_2O + CO_2 \qquad \text{(Eq. 1)}$$

This reaction occurs spontaneously at 518 degrees F (7); however, decomposition of pure sodium bicarbonate begins at temperatures near 100 degrees F (8). The rate is much slower at this lower temperature. Waters (9) has demonstrated that the decomposition of $NaHCO_3$ takes place at temperatures well below 518 degrees F using the fractional thermogravimetric technique. This is illustrated in Figure 1 in which the decomposition of $NaHCO_3$ occurs rapidly at temperatures > 250 degrees F.

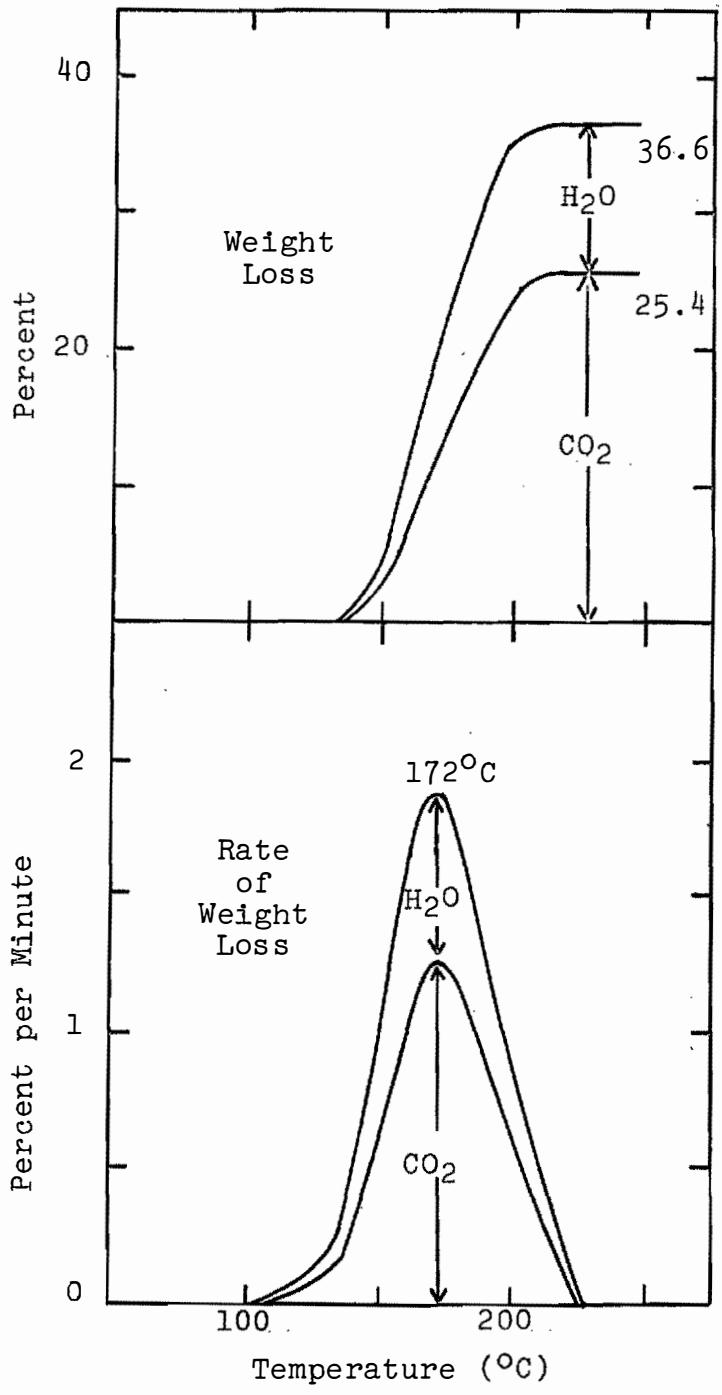

Figure 1. Fractional Thermogravimetric Analysis of $NaHCO_3$ (Heating Rate = 3°C per minute) [reference 8].

The rate of decomposition, as determined by the rate of weight loss in Figure 1, appears to be decreasing at temperatures > 340 degrees F (172 degrees C); this is actually caused by the progressive conversion of the sample.

An important process that accompanies thermal decomposition in $NaHCO_3$ is that of pore development. The Na_2CO_3 particle produced in this manner has a much larger void space than that of the parent $NaHCO_3$ particle. The pores probably provide passageways that facilitate the movement of gas molecules within a particle. Naturally occurring nahcolite is relatively nonporous. Howatson (6) investigated the pore development of raw nahcolite at 300 degrees F with a scanning electron microscope (SEM) and found scattered development of 0.1-0.7μm pores after 10 minutes. After 20 minutes the surface was completely covered with pores averaging about 0.3μm. Heating at higher temperatures produced pores of similar size but their formation was more rapid. The Superior Oil Company (10) reported that the internal surface area of decomposed nahcolite and decomposed sodium bicarbonate was much greater than that of the parent materials. Superior also reported that the greatest internal surface area was generated by decomposing $NaHCO_3$ at temperatures between 250 degrees F and 300 degrees F for minus 200-mesh (74μm) particles. Stern (11), however, found that the maximum

specific surface area was generated by decomposing nahcolite at 600 degrees F in a forced draft oven.

Injection of nahcolite into a very hot environment, such as the flame zone of a boiler, produces thermally crushed Na_2CO_3 (4,10,15). The porous soda ash is produced as at lower temperatures, but the particle size distribution is drastically reduced. For example, the mass mean diameter (MMD) of nahcolite injected into a combustion zone was reduced from MMD=68μm to MMD=1.8μm (4). However, when sustained at temperatures in excess of 600 degrees F the porosity may be reduced by sintering (11).

Another factor, in addition to temperature, that has been found to influence the decomposition rate of $NaHCO_3$ is the size of the particle. Fixed bed data from Superior Oil Company testing indicated that 85% of $NaHCO_3$ particles between 400 and 200-mesh (37 and 74μm) were converted to Na_2CO_3 in approximately 20 minutes (4). In contrast, approximately 70 minutes were required for $NaHCO_3$ particles between 4 and 3 1/2-mesh (4760-5660μm) to reach the same degree of conversion. Figure 2 illustrates this effect.

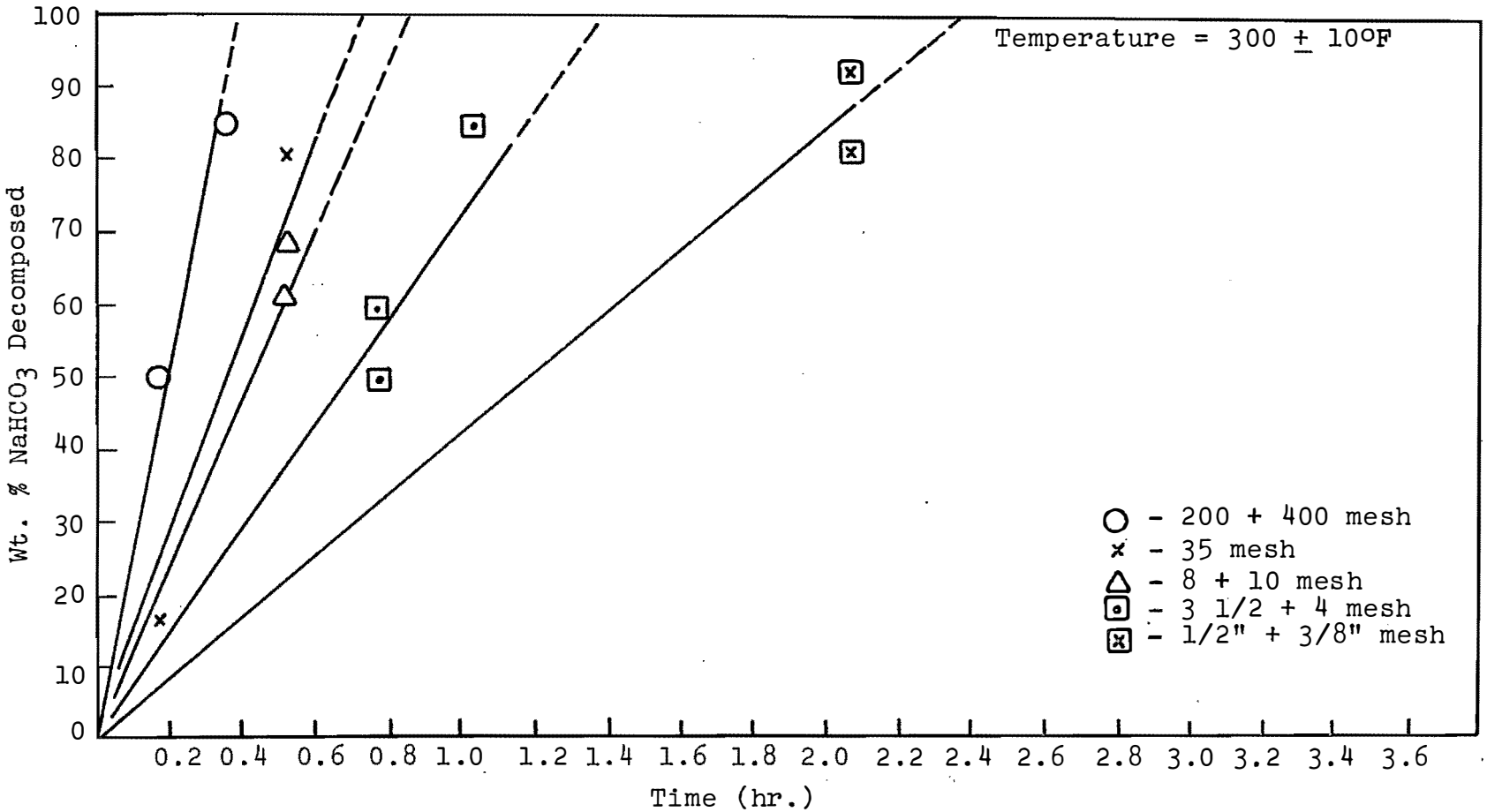

Figure 2. $NaHCO_3$ Decomposition as a Function of Time [reference 10].

Theoretical Reactions

The following desulfurization reactions were postulated by Genco (12) from results obtained in a fluidized bed at approximately 300 degrees F:

$$2NaHCO_3 + SO_2 \rightleftharpoons Na_2SO_3 + 2CO_2 + H_2O \quad \text{(Eq. 2)}$$

$$Na_2CO_3 + SO_2 \rightarrow Na_2SO_3 + CO_2 \quad \text{(Eq. 3)}$$

$$Na_2SO_3 + \tfrac{1}{2}O_2 \rightarrow Na_2SO_4 \quad \text{(Eq. 4)}$$

Note that the combination of Equations 1 and 3 yields Equation 2. Knight reported that for particles larger than 20-mesh (841μm), the decomposition of the $NaHCO_3$ is much faster than the reaction of SO_2 and Na_2CO_3 (10). Some conbination of Equations 2-4 are currently used by most researchers to describe the desulfurization reaction.

Although the investigation of nahcolite as a pollutant control agent was initiated for SO_2 removal, reported values for the removal of nitrogen oxides (NO_x) range from 0-40% (4). The Superior Oil Company reported the results of a series of tests in which the ability of decomposed sodium bicarbonate (Na_2CO_3) to remove NO_x was examined (10). The following reaction was presumed based on the analysis of the data:

$$3NO_2 + Na_2CO_3 \rightarrow 2NaNO_3 + NO + CO_2 \quad \text{(Eq. 5)}$$

Addition of SO_2 to the test gas stream did not produce a major change in NO_2 removal. Tests in the presence of oxygen with NO as the pollutant gas yielded similar results but the solid product was sodium nitrite ($NaNO_2$). Thus, the following reaction was implied:

$$Na_2CO_3 + 2NO + \frac{1}{2}O_2 \rightarrow 2NaNO_2 + CO_2 \qquad \text{(Eq. 6)}$$

Bench Scale Reactors

It is often difficult and expensive to obtain accurate kinetic data from pilot and full scale operations. Also, interpretation of data obtained from bench scale reactors is important in determining what theoretical processes occur during a complex series of reactions like desulfurization. In a fixed bed reactor the gas stream is passed through a stationary layer of sorbent. Three fixed bed experiments and their implications are discussed in this section.

The Superior Oil Company has conducted considerable research into the utilization of nahcolite for SO_2 removal from boiler flue gases. The results of fixed bed tests on decomposed nahcolite were published in 1977 (10). The granular size of the nahcolite varied from approximately 2mm to 13mm. The SO_2 concentration in the flue gas ranged from 450 to 10,000 ppm. The effect of temperatures (from 200-600 degrees F) on reaction rate was also examined.

The large increase in temperature did not influence the rate of reaction. Analysis of the bed material found that sodium sulfate was the ultimate sulfur containing reaction product. Partially reacted particles were examined with a scanning electron microscope (SEM) and a microprobe scan. The SEM micrographs of split particles indicated that a product layer surrounded a more porous core. The microprobe scan determined that the outer layer was composed primarily of sulfate; the inner layer was unreacted. These observations warranted application of the unreacted-core model (13) to the kinetic data. Application of the unreacted core model to chemical kinetic data facilitates the conjecture of a rate controlling step. After applying the unreacted-core model to the reaction rate data, it was concluded that the rate controlling step in the desulfurization process was attributable to ash layer diffusion. Resistance of gas film diffusion and reaction rate were concluded to be negligible. Estimated values for diffusivity of the gas through the ash layer ranged from .001 to .007 cm2/sec for 2000μm particles. [The diffusivity of SO_2 through air at 300 degrees F is approximately 0.27 cm2/sec.] It was noted that the decomposition of nahcolite or sodium bicarbonate occured much faster than the sulfur dioxide substitution for particles > 841 μm; however, decomposition time, in

addition to diffusion, controlled the reaction rate for particles < 841 μm.

Superior Oil used the kinetic data obtained from the fixed bed testing to design a 1000 cfm counter current contactor to remove SO_2 and NO_x (10). SO_2 removal by $NaHCO_3$ is tabulated in Table 2. Nahcolite injection removed up to 40% of the NO_x.

Stern (11) conducted tests to determine the abilities of decomposed nahcolite and trona (another $NaHCO_3$ containing ore) to remove SO_2 and NO. Simulated flue gas was passed through the fixed beds at approximately 10 scfm. The nahcolite was much more effective for SO_2 and NO_x removal than the trona. Decomposition of the nahcolite was affected by placing raw samples into a forced draft oven for 2 hours at a temperature of 600 degrees F. The ore was screened into groups of particles with nominal diameters of 90, 190, and 500 μm. The SO_2 concentration was varied between 500 and 2500 ppm, and the temperature in the reactor was varied from 300 - 750 degrees F. It was determined that maximum utilization of the sorbent for SO_2 removal occurred with smaller sized particles. Utilization improved with increased temperatures up to 650 degrees F, above which the particles sintered and removal decreased. Ninety-eight percent utilization was realized in certain tests under optimum conditions. It was concluded that the

Table 2. SO_2 and NO_x Removal Results with $NaHCO_3$ and Nahcolite Additives

Test Location	Additive	Additive Size	Stoichiometric Ratio	Temperature	SO_2 Removal	NO_x Removal
Superior Counter Current Reactor (9)	$NaHCO_3$	4300 μm	0.86	300°F	84%	
	Nahcolite	3700	0.89	280	67	42%
Owens-Corning (3)	Nahcolite	MMD=13 μm	0.75	300	59	
EPRI (14)	$NaHCO_3$	74 μm	1.00	270	68	0
	Nahcolite		1.00	270	80	0
Grand Forks ETC (15)	Nahcolite	<149 μm			63-77	
University of TN (16)	$NaHCO_3$	MMD=32 μm	1.00	285-315	80	
University of TN (17)	Nahcolite	MMD=14 μm	0.95	350-385	86	
	Nahcolite	MMD=14 μm	0.95	185	17	
Mercer Generating Station (2)	$NaHCO_3$	MMD=60 μm	1.00	600	90	
	$NaHCO_3$	MMD=60 μm	1.00	350	48	
	Nahcolite	MMD=10 μm	1.00	600	94	
	Nahcolite	MMD=10 μm	1.00	350	65	42%*
Nucla Generating Station (10)	Nahcolite		2.0		70	0
Leland Olds Generating Station (9,18)	Nahcolite		1.0	300	73	15

*maximum reported value

reaction was of first order with respect to SO_2 concentration. Nitric oxide adsorption was small and inversely dependent on temperature.

SEM micrographs of halved particles indicated that the desulfurization reaction interface began at the particle perimeter and proceeded inward in the manner described by the unreacted-core model. After applying this model to the data, it was concluded that initially the rate controlling step in SO_2 sorption was the chemical reaction. The rate controlling step was then quickly assumed by diffusion through the product ash layer. Ash diffusion thereafter limited the reaction rate. The diffusivity of the SO_2 through the ash ranged from .0005 to .008 cm2/sec. It was noted that the chemical reaction controlled the rate for low temperatures and small particles.

Hartman (5) concluded that the optimum temperature for desulfurization by Equation 3 was from approximately 250-300 degrees F. The sodium sulfite was oxidized to sodium sulfate (Equation 4) at temperatures > 300 degrees F. It was further concluded that reaction rate was independent of particle size for particles from 200 to 1000 μm.

Pilot Scale Reactors

Although bench scale experiments have provided important data about the removal of pollutants (particularly SO_2) from exhaust gases, pilot scale (and larger) experiments have yielded data that is more useful. That is because research of this latter type is designed to more nearly simulate conditions that are likely to be encountered in operating systems. Sulfur dioxide and NO_x removal values for various pilot systems are listed in Table 2. In contrast to a fixed bed experiment, the dry additive is injected into the system and transported to the fabric filter by the moving gas stream in pilot plant experiments. [The additive was injected continuously throughout each test in the experiments referenced in this section unless otherwise noted.] A typical curve from a pilot plant showing percent SO_2 removal as a function of stoichiometric ratio appears in Figure 3 (18). The location of any point on the curve indicates what removal was obtained at a given set of operating conditions (for example--type and size of adsorbant, system temperature, etc). By changing only one variable (SO_2 concentration in Figure 3), a series of such curves can be used to determine a variable's influence on SO_2 removal. Several pilot scale experiments that illustrate the removal of SO_2 and NO_x under various conditions are discussed in this section.

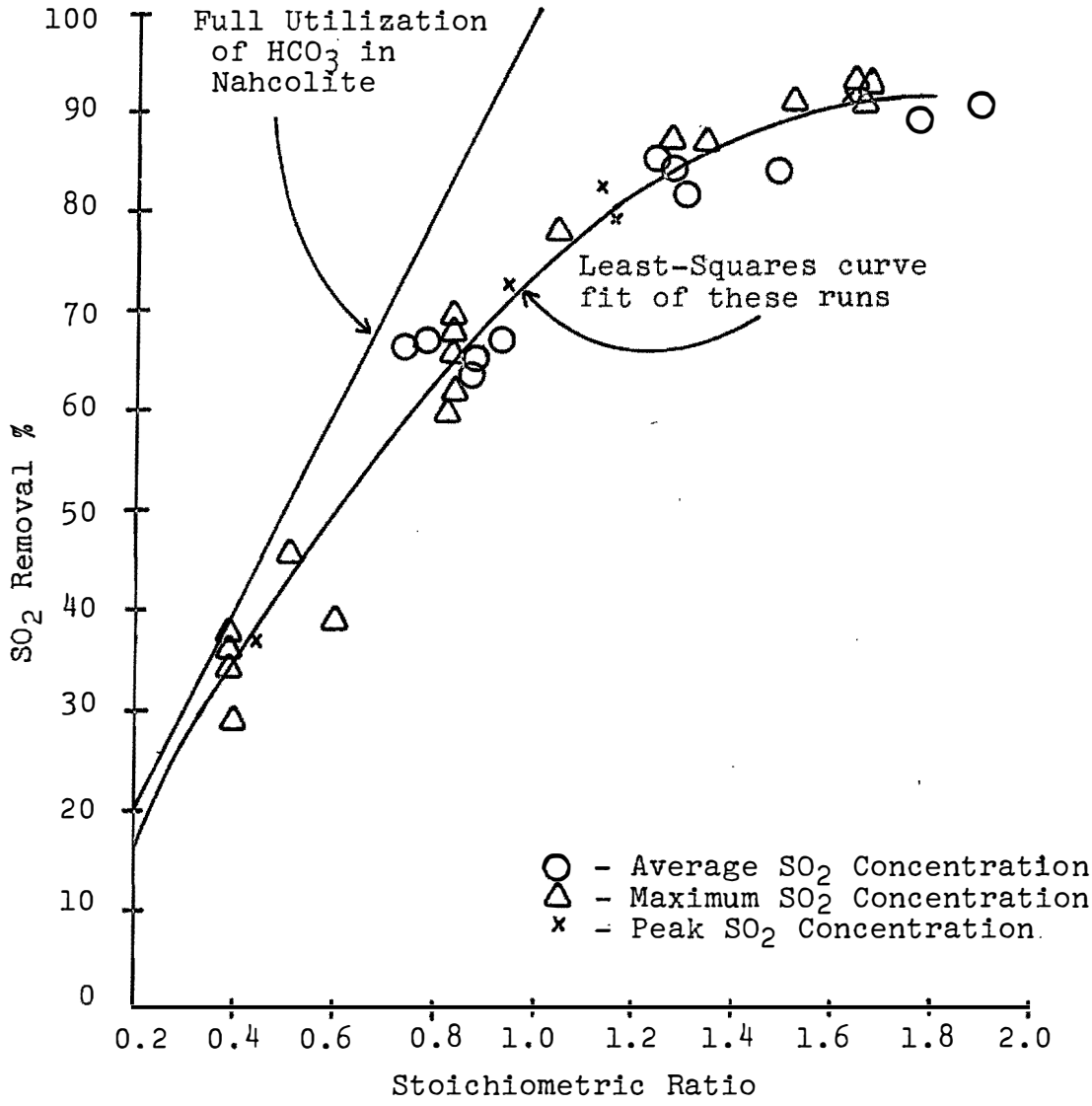

Figure 3. SO_2 Removal as a Function of Nahcolite Stoichiometric Ratio [reference 18].

Veazie and Kielmeyer (3) studied the removal of SO_2 by various sorbents injected into a pilot bag house at Owens-Corning Fiberglass, Inc. The flow rate through the system was varied from 200-600 cfm (3.9-11.7 fpm filtration velocity) and the temperature was varied from 300-1000 degrees F. The SO_2 concentration in the simulated flue gas was maintained at approximately 2800 ppm. Although not the principal sorbent tested, some nahcolite with a mass mean diameter (MMD) of 13 μm was tested at temperatures of 300-500 degrees F. The principal reaction product was sodium sulfate.

Shah and Teixeira (14) conducted SO_2 and NO_x removal studies with $NaHCO_3$, nahcolite, and trona in a nominal 600 scfm bag house. Filtration velocities of 1.3 and 2.2 fpm were used. Two sorbent sizes were injected -- 70% through 200-mesh (74 μm) and 100% through 400-mesh (37 μm). The initial SO_2 concentration was maintained at 400 ppm. The bag house entrance temperature ranged from 255-290 degrees F. The configuration of the system allowed sorbent injection at temperatures of 340 or 530 degrees F. The most effective SO_2 removal was obtained with nahcolite followed, in order of decreasing effectiveness, by $NaHCO_3$ (see Table 2) and trona. Although two air to cloth ratios (1.3 and 2.2) were examined, the results were confounded because the tests were conducted at different temperatures. Thus, no

generalization was appropriate. The introduction of the more finely divided $NaHCO_3$ did not alter the overall SO_2 removal; however the smaller dust exhibited increased removal in the ductwork prior to entering the bag house. It was inferred from analysis of the data that approximately half of the overall SO_2 removal affected by injecting $NaHCO_3$ into the ductwork at 530 degrees F occurred in suspension, with the balance taking place as the gas stream passed through the filter cake. NO_x emissions were not reduced by the injection of any sodium compound tested.

The capabilities of nahcolite and trona as SO_2 removal agents were examined at the Grand Forks Energy Technology Center by Ness and Selle (15). Pilot plant tests were conducted on a 75 lb/hr (130 scfm) pulverized coal-fired furnace with a bag house or an electrostatic precipitator for particulate control. [Only the data obtained with the bag house on line will be used here.] SO_2 flue gas concentrations were in the range of 850-1000 ppm. Decreasing the particle size from 100 to 200-mesh (149 to 74μm) did not effect the amount of SO_2 removed by nahcolite. However, 200 mesh (74μm) trona exhibited an increased capacity for SO_2 sorption over that of the 100 mesh (149μm) trona. The effect of altering the temperature produced no significant change in the desulfurization efficiency, although the researchers noted

that the optimum temperature was about 650 degrees F for SO_2 removal in suspension (that is -- in the ductwork). Injection of the sorbents directly into the flame zone removed approximately 41% of the SO_2 and produced a glassy slag on simulated boiler tubes.

Sodium bicarbonate with a mass mean diameter (MMD) of 31.5 μm was tested as an SO_2 sorbent at the University of Tennessee (16). A portion of the effluent from a stoker coal-fired boiler was utilized in a 100 cfm bag house. Although the pilot plant had a nominal flowrate of 100 cfm, the filtration velocity was varied from 2.5-5.0 fpm for test purposes. The bag house temperature was approximately 300 degrees F and the SO_2 concentration of the flue gas ranged from 700-3000 ppm. Varying neither the filtration velocity over the range of 2.5-5.0 fpm nor the SO_2 concentration over the range of 700-3000 ppm had any significant effect on the overall SO_2 removal by $NaHCO_3$ at stoichiometric ratios of 0.5 to 2.0.

Nahcolite (MMD=14-27 μm) and $NaHCO_3$ (MMD=32 μm) were examined as SO_2 removal agents in a 1000 acfm pilot bag house system at the University of Tennessee (17). This unit was also arranged so that a slipstream was supplied from a stoker coal-fired boiler flue gas duct. The filtration velocity was 3 fpm. The bag house temperature was varied from 100-350 degrees F. The SO_2 removal that resulted from $NaHCO_3$ injection was similar to

the data obtained on the smaller unit at 300 degrees F (see Table 2); however, the nahcolite was more effective at 350 degrees F. This was attributed to one or more of the following causes: the smaller size of the nahcolite, the higher bag house temperature in the nahcolite series of tests, and, since only the $NaHCO_3$ fraction was assumed to react with SO_2, to the non-bicarbonate fraction of the nahcolite. It was observed that an increase in the bag house temperature augmented nahcolite's SO_2 removal capacity (see Table 2). Under optimum conditions, nahcolite removed up to 70 % of the SO_2 present in the ductwork before entering the bag house (1.75 seconds of residence time).

Liu and Chaffee (2) examined the removal of SO_2 (and NO_2 to some extent) by lime, nahcolite (MMD = 10 μm), and $NaHCO_3$ (MMD = 60 μm) in a top entry pilot baghouse built by Air Preheater Co. at Mercer Genorating Station of Public Service Gas and Electric Co. of New Jersey. [All the other pilot plants in this section used bottom entry bag houses.] Only the results of $NaHCO_3$ and nahcolite testing are discussed here. Either the additive was injected continuously throughout a test or the amount of additive required for an entire test was added in a "batch" during the initial period of a test. The difference in SO_2 removal between tests with different injection methods was slight. The gas flow rate through

the system was varied from 7500-15000 acfm (filtration velocities of 1.7 to 3.8 fpm depending on operating conditions). Tests were conducted in three approximate temperature regimes: 270 degrees F, 350 degrees F, and 600 degrees F. The SO_2 concentration varied during each test but averaged from 800-1500 ppm; the NO_2 concentration varied from 800-1100 ppm. The velocity of the gas stream through the system was found to have a slightly negative effect on SO_2 removal by both $NaHCO_3$ and nahcolite. Davis et al. thought that this might be due to the decreased filter cake that accrues in top entry bag houses at higher filtration velocities (16). Since less of the sorbent is deposited on the fabric surface at higher velocities, there is less sorbent on the fabric surface to react with the SO_2. The strongest influence on SO_2 removal efficiency by the sodium additives was that of temperature (2). $NaHCO_3$ removal at a stoichiometric ratio of 1.0 increased from 48% to 90% with a temperature increase of 350 to 600 degrees F; nahcolite removal increased from 65% to 94% at the same respective temperatures and stoichiometry. Both additives exhibited similar behavior in suspension. Approximately 13% of the total removal took place in the duct at 270 and 350 degrees F; 63% of the total removal occurred in the duct at 600 degrees F. Although the overall SO_2 removal by nahcolite appeared to be greater than that of $NaHCO_3$ at

the same stoichiometric conditions, the additives could not be directly compared for the following two reasons: firstly, since the nahcolite was composed of 70% $NaHCO_3$, the mass rate at which it was injected was larger than that of the pure $NaHCO_3$ at the same stoichiometric ratio, and secondly, the nahcolite (MMD = 10 μm) was much smaller than the $NaHCO_3$ (MMD = 60 μm). Some testing was conducted to determine whether NO_2 was removed along with the SO_2. Although a maximum NO_2 reduction of 42% was achieved with nahcolite injection at 350 degrees F, the average NO_2 removal of the tests was approximately 15%.

A large pilot plant was constructed at the Nucla Station of the Colorado Ute Electric Association by Wheelabrator-Frye, Inc. (4). The gas flowrate through the system was 65000 acfm at a filtration velocity of 2.0-3.0 fpm. Nahcolite was injected into the system by the "batch" method outlined above. The SO_2 concentration in the inlet flue gas was 400-500 ppm. Varying the filtration velocity had no significant effect on SO_2 removal. No NO_x was removed by the nahcolite. The product of the desulfurization reaction was found to be primarily Na_2SO_4. Although instantaneous SO_2 removal efficiencies of > 90% were observed, the reported removal was determined by averaging the values obtained from an entire test. This was done to determine whether or not federal emission limits could be met by using the "batch"

method of injection. The 70% removal required was attained at a stoichiometric ratio of 2.0.

Wheelabrator-Frye also conducted dry SO_2 and NO_x adsorption studies in conjunction with the Superior Oil Company and Bechtel Power Corp. at Basin Electric Power Cooperative's Leland Olds Station (10,18). Nahcolite, supplied by Superior Oil Co., was injected by both "batch" and continuous methods into the 3100 acfm bag house. The filtration velocity was 3 fpm in the system. The SO_2 inlet concentration was varied from approximately 800-2800 ppm, but this variation did not alter the SO_2 removal efficiency attained at any given stoichiometric ratio.

Summary

The removal of SO_2 and NO_x by $NaHCO_3$ and nahcolite has been studied in both bench scale and pilot scale experiments. These experiments differed both in physical design and in the additive preparation procedure. Bench scale research has been conducted on decomposed $NaHCO_3$ or nahcolite in fixed beds. Pilot scale research has generally been done by injecting raw $NaHCO_3$ or nahcolite into the ductwork upstream of a bag house.

Decomposing the additive before testing its SO_2 or NO_x removal capabilities eliminated one of the chemical reactions (Equation 1) that would have occurred during testing at typical flue gas temperatures. Thus, using the fixed bed technique, the desulfurization reaction (as

explained by Equation 3) has been mathematically modeled. This technique, in addition to SEM analysis of the reaction product, has indicated that SO_2 is removed by the gas/solid reaction scheme described by the unreacted-core model. Although not studied extensively, no appreciable NO_x has been shown to be removed by decomposed $NaHCO_3$ or nahcolite.

Various SO_2 and NO_x removal values have been reported in pilot scale systems. At a stoichiometric ratio of approximately 1.0 and temperatures of 270-350 degrees F, the following results were obtained (from Table 2): 48 to 80% SO_2 removal by $NaHCO_3$, 65 to 94% SO_2 removal by nahcolite, and 0 to 40% NO_x removal $NaHCO_3$ and nahcolite. This wide range of values can be partly explained by noting that the operating variables (such as gas velocity, temperature, particle size, and SO_2 or NO_x concentration) varied from system to system. Although SO_2 removal was generally shown to be dependent on temperature, the effects of other variables were disputed.

This research effort was undertaken to examine the effects of additive preparation and additive size on the removal of SO_2 and NO by $NaHCO_3$ in a pilot scale system. This was done by comparing the removal results of raw and decomposed $NaHCO_3$ dusts of different sizes.

II. THEORETICAL CONSIDERATIONS

General Comments

The removal of a pollutant gas from an effluent by additive injection into a bag house system is complicated. In the case considered here, the additive is injected into the ductwork on the upstream side of a bottom feed bag house at a temperature > 250 degrees F. The following series of events occur: initially, the injected additive is fluidized by the moving gas stream; then, the additive travels concurrently with the gas stream to the filtration surface; and lastly, the gas stream passes through the stationary filter cake. The system thus functions as a series of three reactors -- a fluidized bed, a cocurrent contactor, and a fixed bed. By assuming that the reactions discussed in the previous section (Equations 2-4) are responsible for the removal of SO_2 by $NaHCO_3$ and Na_2CO_3, a sequence of steps can be postulated that describe the interaction between a single additive particle injected into the system and the SO_2 laden gas stream:

1. If the particle is $NaHCO_3$, it begins to decompose into Na_2CO_3, H_2O, and CO_2.
2. SO_2 diffuses through the boundary film surrounding the particle toward the particle surface.

3. SO_2 diffuses through the particle pore space to the solid surface.

4. A SO_2 molecule is adsorbed onto the surface and reacts with the additive.

5. The gaseous products of the reaction desorb and diffuse back through the pore space.

6. The reaction products diffuse back through the boundary film.

The hierarchy of events discussed above can perhaps be best envisioned by application of the unreacted-core model. In the unreacted-core model the reaction is assumed to occur initially at the outer surface of the particle. The zone of reaction moves toward the center of the particle leaving a layer of solid reactant behind (as illustrated in Figure 4 [from reference 13]). This model is probably the best simple representation available for most gas/solid systems. Also, SEM and microprobe analyses of desulfurization products, after the exposure of Na_2CO_3 to a SO_2 containing gas stream, have revealed the existence of a layer of Na_2SO_4 around a virtually pure core of additive. The six steps listed in the previous paragraph can be considered to exist in series. This is frequently done in non-catalytic heterogeneous systems (7). If viewed in sequence, the total time for any degree of conversion is equal to the sum of the times required for each step, that is:

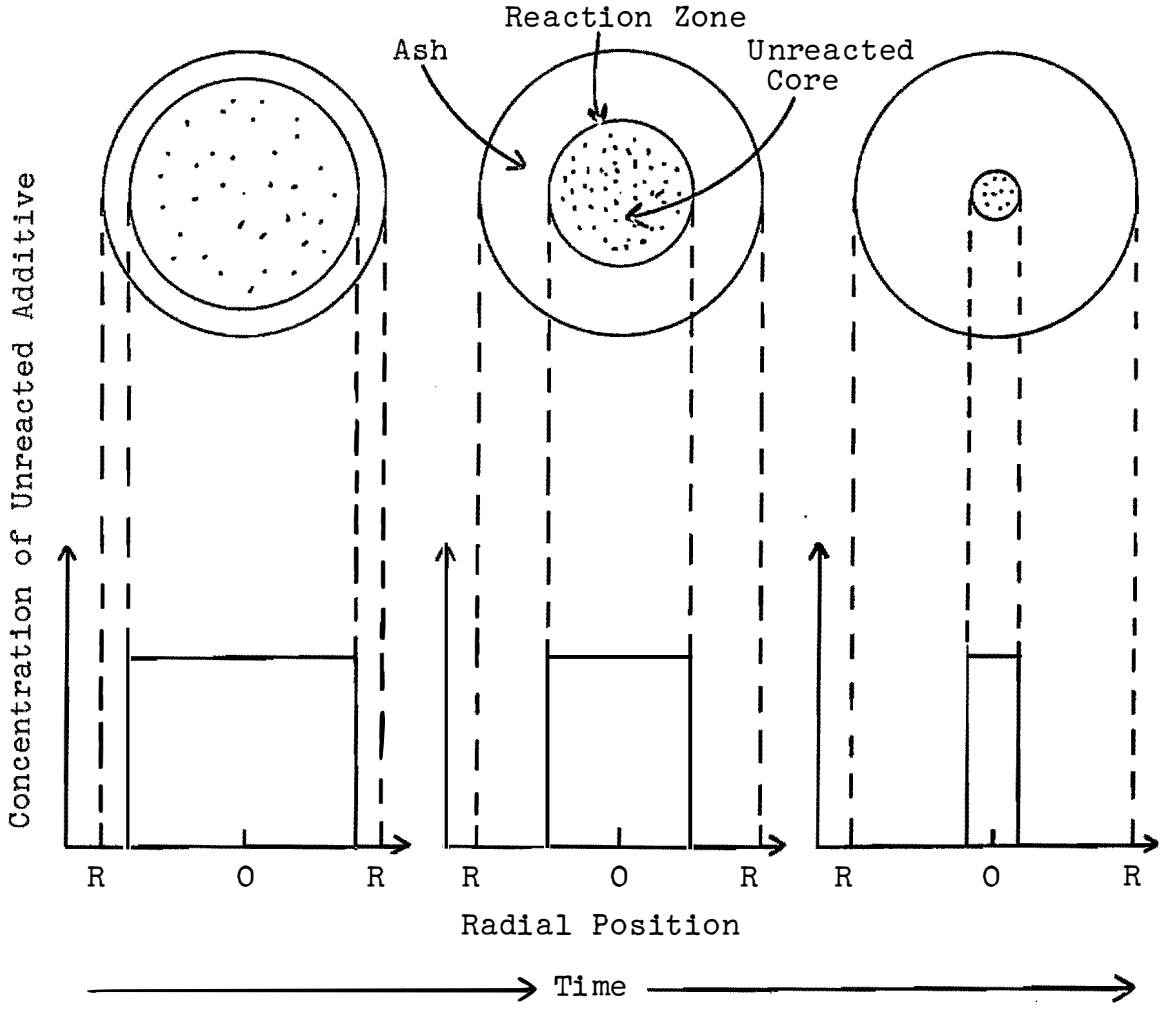

Figure 4. The Zone of Reaction is Assumed to Move from the Surface Toward the Center of a Particle in the Unreacted-Core Model [reference 13].

$$t_{total} = t_{decomposition} + t_{film\ diffusion} + t_{ash\ diffusion} + t_{reaction}$$

If one step is appreciably slower than the others, that step is effectively rate limiting and

$$t_{total} \approx t_{limiting\ step}$$

The unreacted-core model defines the operations of film diffusion, ash layer diffusion, and chemical reaction as those with potential rate controlling capabilities.

<u>The Unreacted-core Model</u> (after 13)

case 1 -- Diffusion Through the Gas Film Controls

When diffusion through the gas film is limiting, the rate at which gas A is utilized is controlled by the mass transfer of A across the boundary film. As illustrated in Figure 5, the bulk concentration of A (CAg) in the gas stream outside the gas film is constant. Since the rate of diffusion through the ash layer and the rate of reaction are much faster than the rate of gas film diffusion, the concentrations of A at the particle surface (CAs) and at the reaction interface (CAc) are very small. The equation describing this transfer is:

$$\frac{dNA}{dt}\left(\frac{1}{S}\right) = -\mathcal{D}_G \left(\frac{dCA}{dz}\right)_{gas} \qquad \text{(Eq. 7)}$$

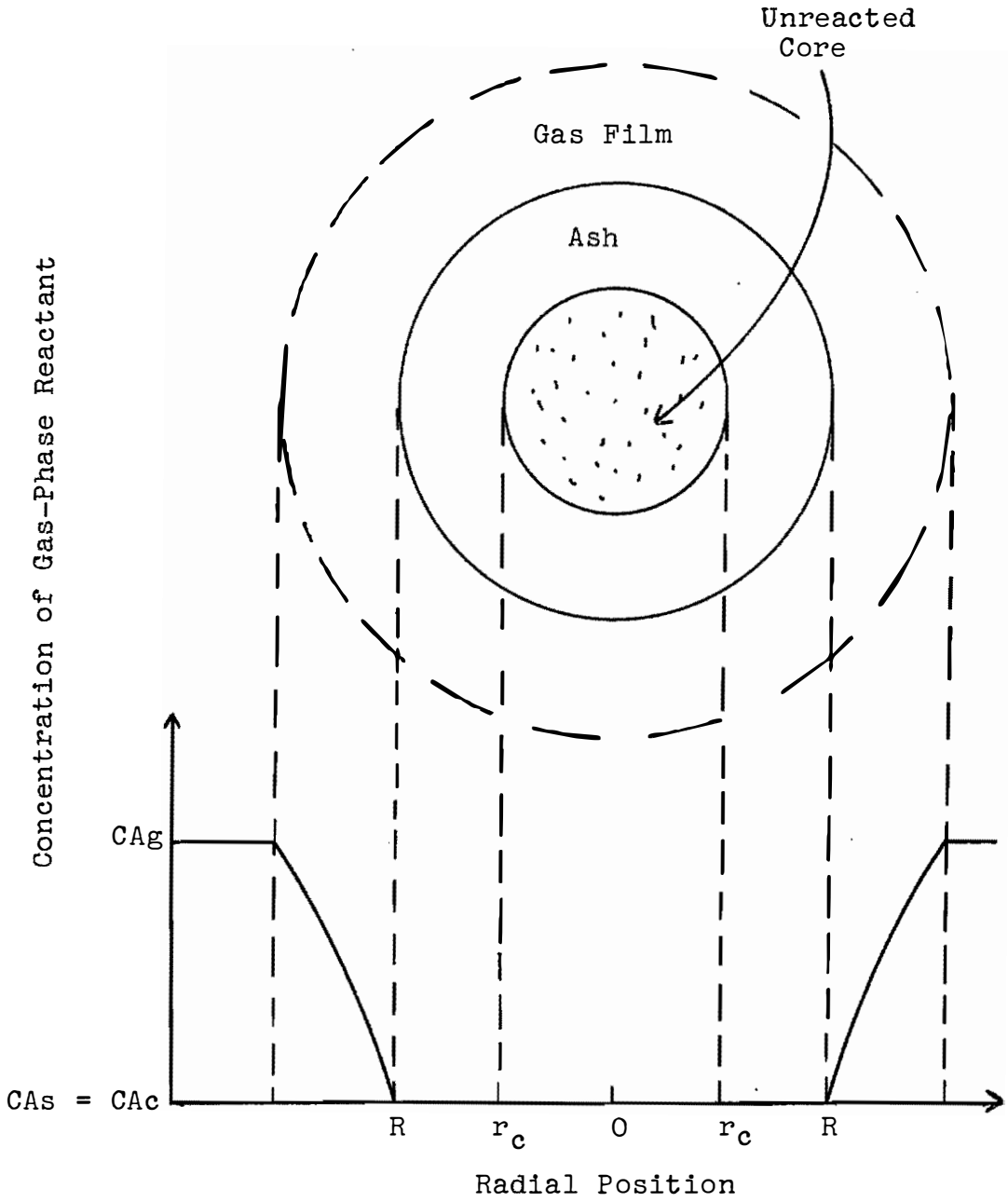

Figure 5. Diffusion Through the Gas Film Controls [reference 13].

where $\frac{dNA}{dt}$ = rate of molar transport of A($\frac{moles}{t}$)

S = area perpendicular to the diffusion path (L^2)

$\mathcal{D}_G$ = diffusion coefficient of A through the gas film ($\frac{L^2}{t}$)

$(\frac{dCA}{dz})_{gas}$ = concentration gradient of A across the gas film of thickness dz.

case 2 -- Diffusion Through the Ash Layer Controls

When diffusion through the ash layer is limiting, the rate at which gas A is utilized is controlled by the mass transfer of A through the pore space of the ash layer. Because the rate of diffusion through the ash layer is much larger than either the rate of gas film diffusion or the rate of reaction, the conditions depicted in Figure 6 exist. The bulk concentration of A (CAg) in the gas stream is the same as that on the particle surface (CAs). The concentration of A at the reaction interface (CAc) is very small. The equation describing this transfer is:

$$\frac{dNA}{dt}\left(\frac{1}{S}\right) = -\mathcal{D}_{ash}\left(\frac{dCA}{dz}\right)_{ash} \qquad \text{(Eq. 8)}$$

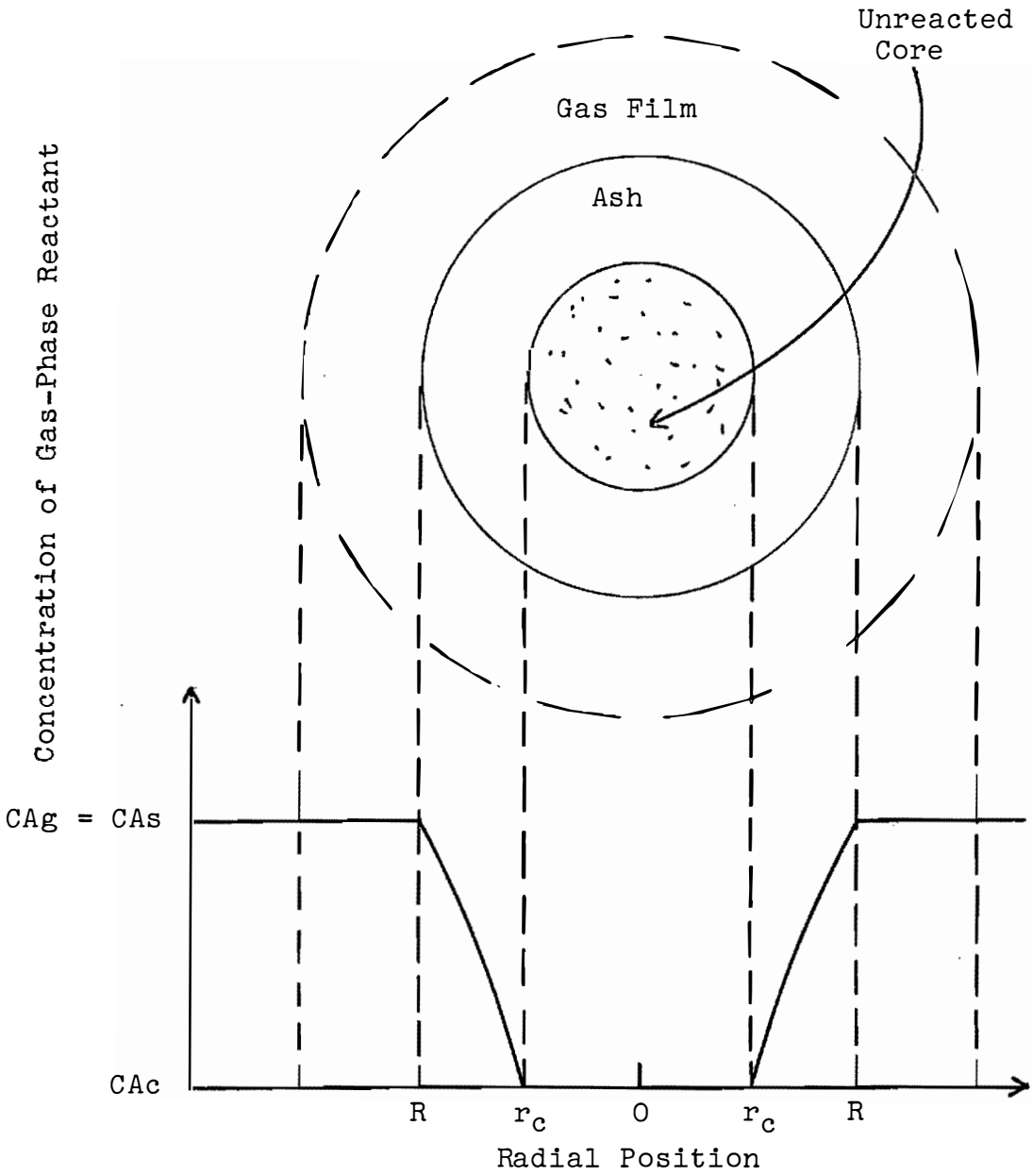

Figure 6. Diffusion Through the Ash Layer Controls [reference 13].

where $\frac{dNA}{dt}$ = rate of molar transport of A($\frac{moles}{t}$)

S = area perpendicular to the diffusion path (L^2)

$\mathcal{D}_{ash}$ = diffusion coefficient of A through the ash layer ($\frac{L^2}{t}$)

$(\frac{dCA}{dz})_{ash}$ = concentration gradient of A across the ash layer of thickness dz

case 3 -- Chemical Reaction Controls

If the utilization of A is not dependent on the transfer of the gas A to the reaction site (solid reactant/solid product interface), then the reaction rate limits the overall rate. Figure 7 shows that the concentration of A is essentially constant in the bulk phase, through the gas film, and through the ash layer -- CAg=CAs=CAc. The concentration of A at the reaction interface (CAe) is very small. Thus the general relationship

$$aA_{gas} + bB_{solid} \rightarrow \text{products}$$

is described by the following equation:

$$\frac{dNA}{dt}\left(\frac{1}{S}\right) = -K_S C_A^a C_B^b \qquad \text{(Eq. 9)}$$

where $\frac{dNA}{dt}$ = rate of conversion of A($\frac{moles}{t}$)

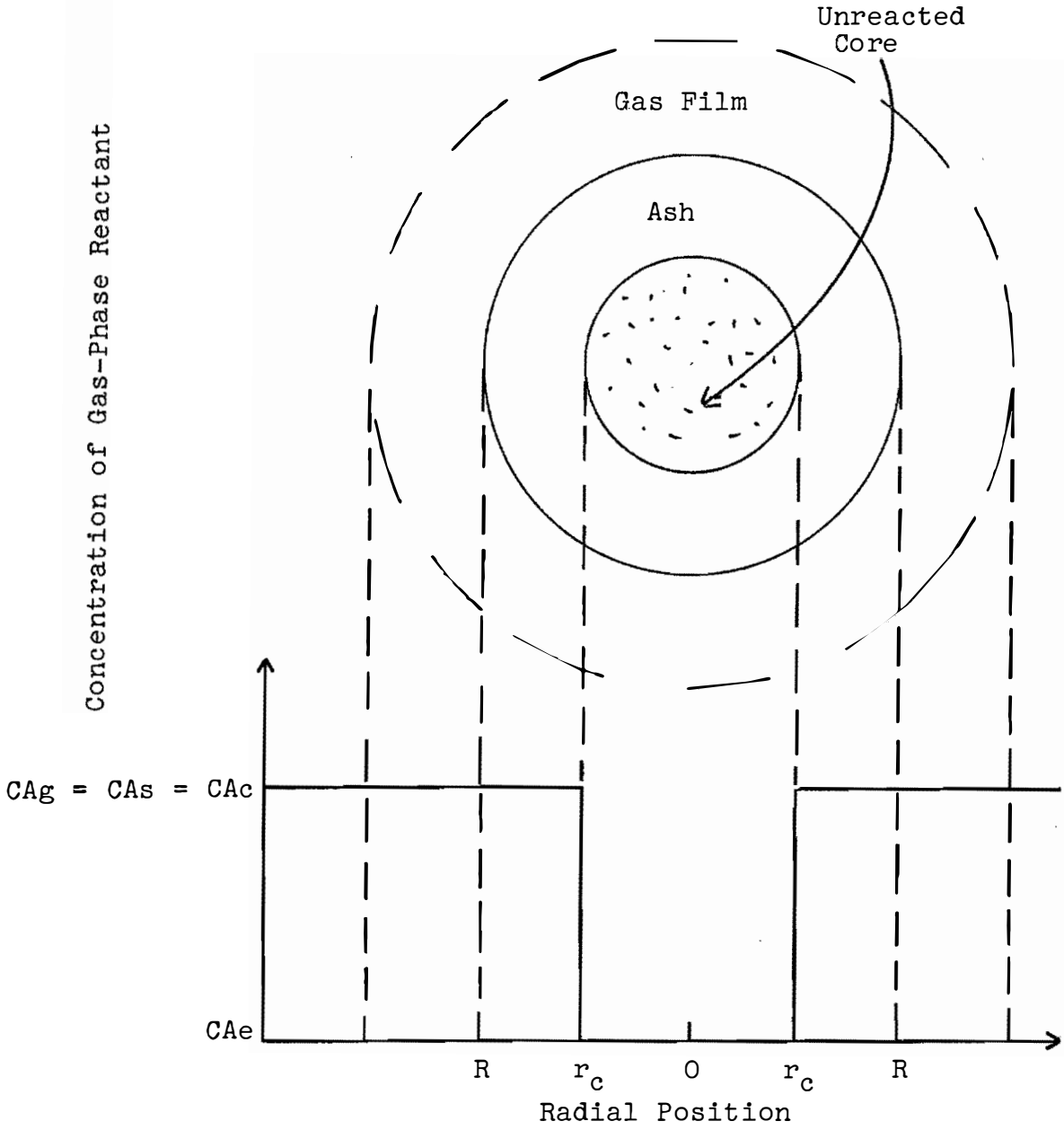

Figure 7. Chemical Reaction Controls [reference 13].

S = area of reaction zone (L^2)

K_S = reaction rate coefficient

C_A, C_B = concentration of component at reaction site ($\frac{moles}{L^3}$)

a, b = stoichiometric coefficients

n = reaction order = $a + b$

Determination of the Rate Controlling Step

The rate controlling step can be determined experimentally in the following four different ways:

a. Utilizing integrated forms of Equations 7-9, predicted and actual data can be compared. If one equation describes the overall reaction more accurately than the others, control by that step is implied (13).

b. The rate of chemical reactions are inherently much more sensitive to temperature changes than those of physical processes. A marked variation in reaction rate with temperature indicates chemical reaction control (7, 13).

c. Mass transfer, specifically gas film diffusion, is dependent on the velocity of the gas stream moving past a particle. If an increase in the overall rate is obtained from augmenting the

velocity, control by gas film diffusion is implied (7).

d. Decreasing the particle size tends to increase the rates of both mass transfer and chemical reaction. However, this effect is much more pronounced on the mass transfer steps than on the chemical reaction step. Consequently, if the overall reaction rate is significantly increased by utilizing a smaller particle, mass transfer (film and/or ash layer diffusion) probably control (7, 13).

It should be noted that in real systems the controlling steps may actually change during the course of a reaction. In addition, Figure 8 illustrates how that a change in a variable can alter the controlling process (19). For a large particle, the controlling process can be either chemical, diffusional, or mixed depending on the temperature. Also, at a fixed temperature either diffusion, mixed, or chemical control will be predominant, depending on the particle size. Lastly, the removal of SO_2 by $NaHCO_3$ cannot be completely represented by the unreacted-core model, due to the rapid decomposition of $NaHCO_3$ at temperatures > 250 degrees F.

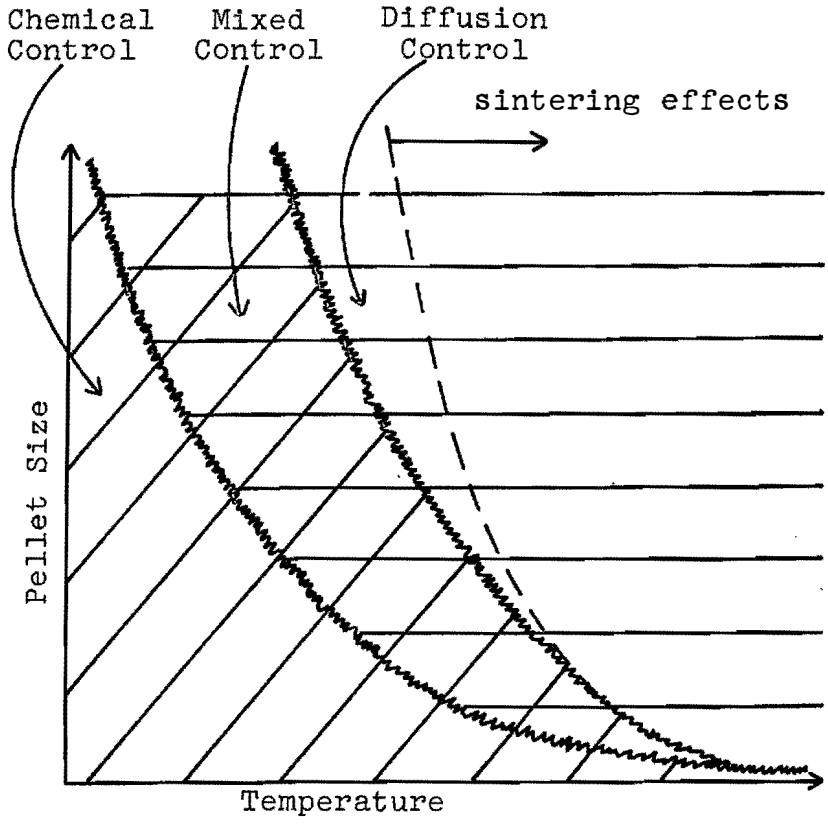

Figure 8. Representation of How Temperature and Particle Size Determine the Rate-Controlling Step [reference 19].

III. EXPERIMENT DESIGN

Description of the Test Facility

The fabric filter collector was installed on a Riley spreader-stoker coal-fired boiler located at the University of Tennessee at Knoxville. At 100% capacity the boiler produced 100,000 pounds of steam per hour. Steam production was typically 30-60% of capacity. A slip stream of 963 acfm was removed from the main ductwork downstream of a multiple cyclone with a particulate removal efficiency of approximately 90%. The particulate loading in the sample stream was approximately 0.16 grains/acf as determined by EPA Source Sampling Method Five. Analyses of a typical coal ash sample yielded the following weight percentages of various compounds:

Sulfur	1.6%
SiO	7.8%
Al_2O_3	4.2%
Fe_2O_3	2.0%
CaO	0.1%
MgO	0.2%
Na_2O	0.05%
K_2O	0.6%
Total ash	16%

The slip stream was pulled through the pilot system by an induced draft fan. The system layout is represented schematically in Figure 9. The ductwork contained ports that permitted the injection of water, ambient air , additional SO_2, and powdered additives. Other ports were provided for sampling SO_2 and NO concentrations before any additive was injected, at three positions in the ductwork upstream of the bag house, and at one position downstream of the bag house. Finally, ports were installed that facilitated stack sampling operations such as the determination of the gas flow rate, the system particulate loading, and bag house efficiency. At the tested filtration velocity of 2.5 fpm, the average velocity in the duct was 2600 fpm. This produced a residence time of 2.0 seconds between the site of additive injection and the bag house hopper. Duct temperatures at the additive inlet were approximately 300 degrees F in the low temperature tests and 375 degrees F respectively. The temperature in the system was lowered by the addition of ambient air. The SO_2 concentration in the sample stream ranged from 500-800 ppm but was increased to 1000-3000 ppm via the injection of bottled anhydrous SO_2.

The bag house consisted of one filtration compartment containing four 32 ft. x 11.25 inch fiberglass bags (14.5 oz/yd2). The system was operated manually or automatically. The dust cake was removed from

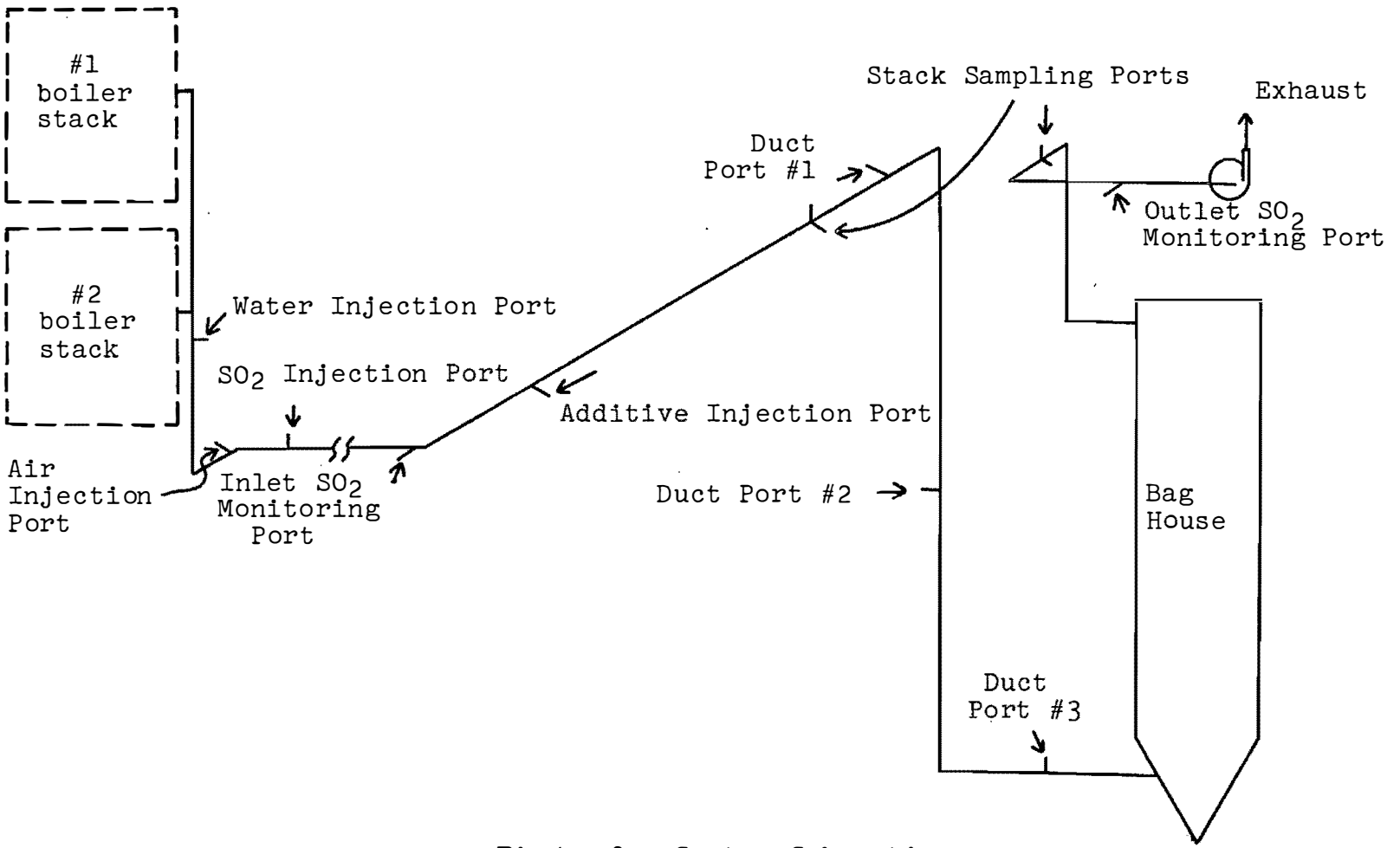

Figure 9. System Schematic

the inner bag surface by shaking. In the automatic mode, cleaning occurred once an hour and the hopper was emptied during this cleaning period by a rotary valve located beneath the hopper. Manual operation of the system allowed initiation of the cleaning cycle at any time. The rotary valve was operable independently of the shaking mechanism, allowing collection of the hopper fallout and bag cake separately. The overall particulate removal of the system on flyash was > 98.6% as determined by EPA Source Sampling Method Five.

Test Procedures

The capabilities of ten additives to remove SO_2 and NO were studied; these were five $NaHCO_3$ samples and five Na_2CO_3 samples. The $NaHCO_3$ samples were five commercially available powders provided by the Church and Dwight Co, Inc. The five Na_2CO_3 dusts were obtained by heating 10 pound samples of the five $NaHCO_3$ dusts in a 350 degree F oven for 8 hours. At the end of this period, the weight of the samples indicated that the samples had been completely converted to Na_2CO_3 (as determined from Equation 1). Chemical analyses of the samples verified that the raw $NaHCO_3$ samples were > 99% pure bicarbonate, and that the Na_2CO_3 samples were > 99% pure carbonate. The analytical technique used appears in Appendix A. The size distribution of the additive samples was determined from a combination of Coulter Counter and Ro-Tap sieve

analyses. These analyses are tabulated in Appendix B. The estimated mass mean diameters of the samples are listed in Table 3. Where the Coulter Counter and sieve analyses differed, the Coulter Counter analysis was used.

It was intended that the following data be obtained for each test (a detailed description of the equipment used can be found in Appendix C):

1. SO_2 concentration (inlet and outlet) -- Dyna-Sciences SO_2 monitor.
2. NO concentration (inlet and outlet) -- Lear Siegler SO_2/NO monitor.
3. O_2 and CO_2 concentrations -- Bacharach Fyrite Analyzers.
4. Percent water vapor in the flue gas -- psychrometry.
5. Additive feed rate -- Vibrascrew adjustable feeder.
6. Duct and bag house temperatures -- calibrated thermometers.
7. Local barametric pressure -- mercury barometer.

Cylinders of certified SO_2 and NO were used to calibrate the gas analyzers. NO was not measured in all tests due to mechanical difficulties with the analyzer. Filtered, heated sample lines were installed for the purpose of monitoring the SO_2 concentration before any additive was injected (inlet), on the clean side of the bag house

Table 3. Additive Characteristics

Additive	Mass Mean Diameter Coulter Counter	Mass Mean Diameter* U.T. Seive Analysis	Mass Mean Diameter* Church and Dwight	Bag House Hopper Collection Efficiency (by mass)
Sodium Bicarbonate #3DF	32 μm		33 μm	9%
Sodium Bicarbonate #1	52 μm	67 μm	58-71 μm	30%
Sodium Bicarbonate #2		119 μm	132-145 μm	38%
Sodium Bicarbonate #4		154 μm	<140 μm	
Sodium Bicarbonate #5		193 μm	230 μm	50%
Soda Ash #3DF	27 μm			
Soda Ash #1	42 μm	69 μm		5%
Soda Ash #2		94 μm		36%
Soda Ash #4		101 μm		50%
Soda Ash #5		180 μm		50%

*estimated from log probability plots

(outlet), and at three locations in the ductwork downstream of the additive port. However, data obtained in the duct were not reliable, due to the fact that in some instances some SO_2 was removed by the additive in the sampling system itself. For this reason, no further attempt was made to monitor SO_2 removal in the ductwork. No difficulty was encountered in monitoring the inlet and outlet concentrations since there was no additive present at those locations.

The stoichiometric ratio was determined by the molar rates of additive and SO_2. The molar rate of additive injection was determined from the gravimetric feed rate of the Vibrascrew feeder. The molar flow rate of SO_2 was determined from the SO_2 concentration, the gas density, and the gas flow rate. A similar procedure was employed to determine a Na/NO equivalent ratio. The calculation procedures appear in more detail in Appendix D. It was originally intended that all testing should be conducted at 1000 ppm SO_2 and with an appropriate additive feed rate to produce a stoichiometric ratio of 1.0. This was not feasible for two reasons. Firstly, the SO_2 concentration in the main boiler system often varied from minute to minute. Since the additive was fed at a constant rate, the stoichiometric ratio often changed during the course of a test. Secondly, due to the different natures of the additives, it was not always

possible to inject a given additive at the proper rate to ensure a stoichiometric ratio of 1.0. To obtain a stoichiometric ratio as near to 1.0 as possible, it was necessary to vary the inlet SO_2 concentration by adjusting the rate of anhydrous SO_2 injection.

The percent SO_2 and NO removal efficiencies were determined from the inlet and outlet concentrations from the following relationships:

$$\eta = (1 - \frac{c_{out}}{c_{in}}) \times 100\%$$

$$P_{en} = 100\% - \eta$$

where η = percent removal efficiency

c_{out} = outlet gas concentration (ppm)

c_{in} = inlet gas concentration (ppm)

P_{en} = percent penetration

Since the SO_2 concentration often fluctuated during the course of a run, the removal efficiency was computed when the outlet SO_2 concentration approached a constant value. The corresponding removal efficiencies and stoichiometric conditions were recorded at that time. It would have been desirable to also determine the efficiency on a total or integrated basis; however, the inherent variations in the system prevented this. All efficiency data were thus determined at conditions approaching a steady state.

The hopper fallout and the filter cake were collected separately in certain tests. The total weight for each fraction was determined and a sample was tightly sealed and retained for analyses. The weight percent collected in the hopper was used to determine the collection efficiency of the hopper. This efficiency was plotted as a function of mass mean diameter for the materials tested (Figure 10). As anticipated, the hopper efficiency increased with the injection of larger additives. Some of the ash samples were analyzed for total sulfur by a Fisher 470 Total Sulfur Analyzer and for bicarbonate/carbonate by the technique in Appendix A. Determination of the total sulfur present in the hopper and filter cake samples allowed calculation of the percent SO_2 removed by each fraction. The calculation procedure used is included in Appendix D.

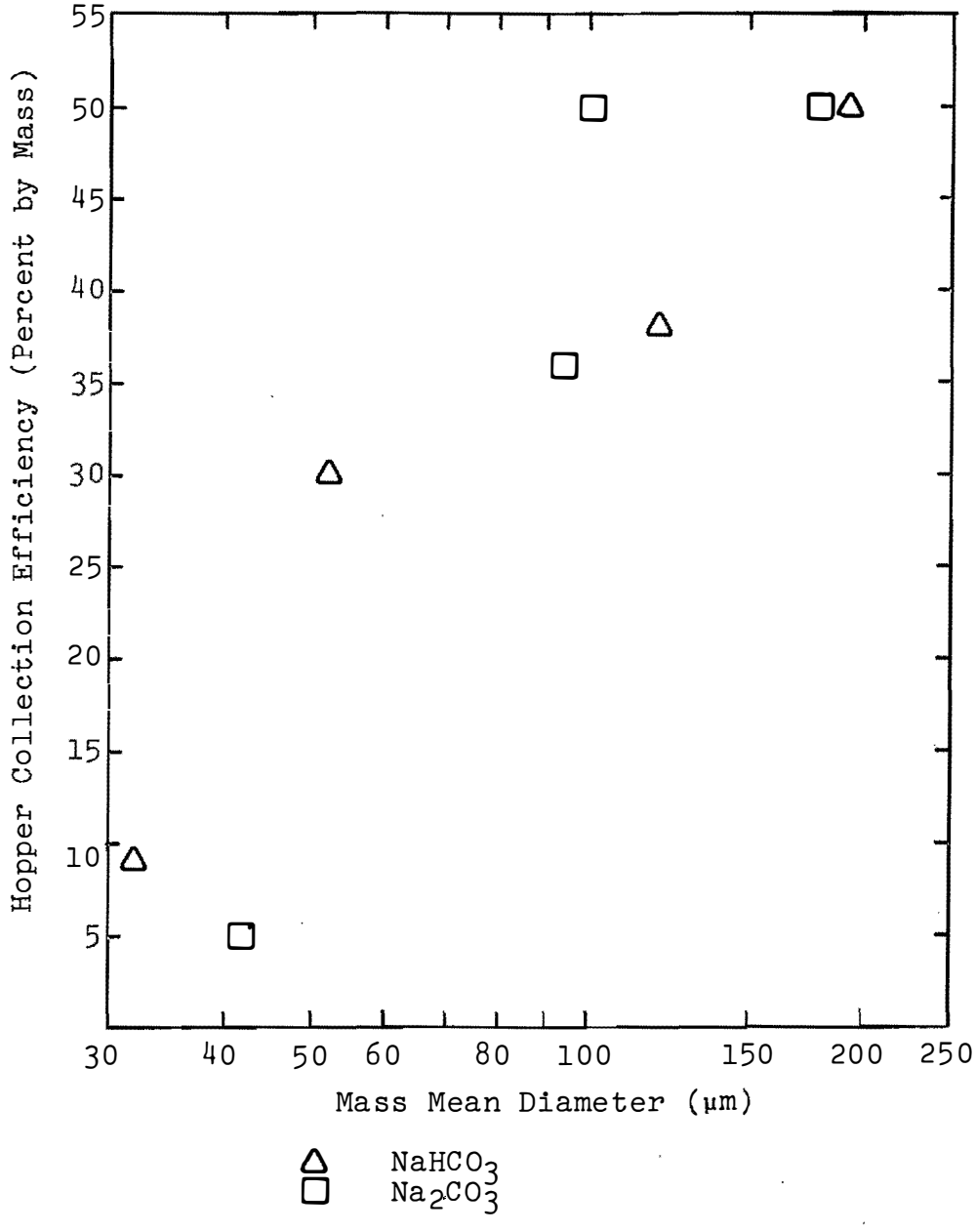

Figure 10. Collection Efficiency of the Bag House Hopper as a Function of Additive Mass Mean Diameter.

IV. RESULTS AND DISCUSSION

SO_2 Removal by Flyash

The ability of flyash to remove SO_2 has been demonstrated. However, flyash alone (no additive injection) removed < 5% of the SO_2 present when tested, probably due to the small particulate loading (0.16 gr/acf). SO_2 removal by flyash was assumed to be equal to zero percent for calculation purposes.

SO_2 Removal by $NaHCO_3$

Nine separate tests were performed to evaluate the effect of particle size, represented by mass mean diameter, on SO_2 removal by $NaHCO_3$. These tests were conducted in the two temperature regimes discussed previously; duct and bag house temperatures were approximately 375 and 300 degrees F, respectively, in the high temperature tests and 300 and 250 degrees F, respectively, in the low temperature tests. Stoichiometric ratios ranged from about 0.5 to 1.5. The mass mean diameters of the five dusts are listed in Table 3. The results and specific test conditions are tabulated in Appendix E. A graphical presentation of these results appears in Figure 11, in which the total SO_2 removal of the system is plotted as a function of additive stoichiometric ratio. [Data obtained from previous tests of SO_2 removal by 32μm MMD $NaHCO_3$, at similar conditions

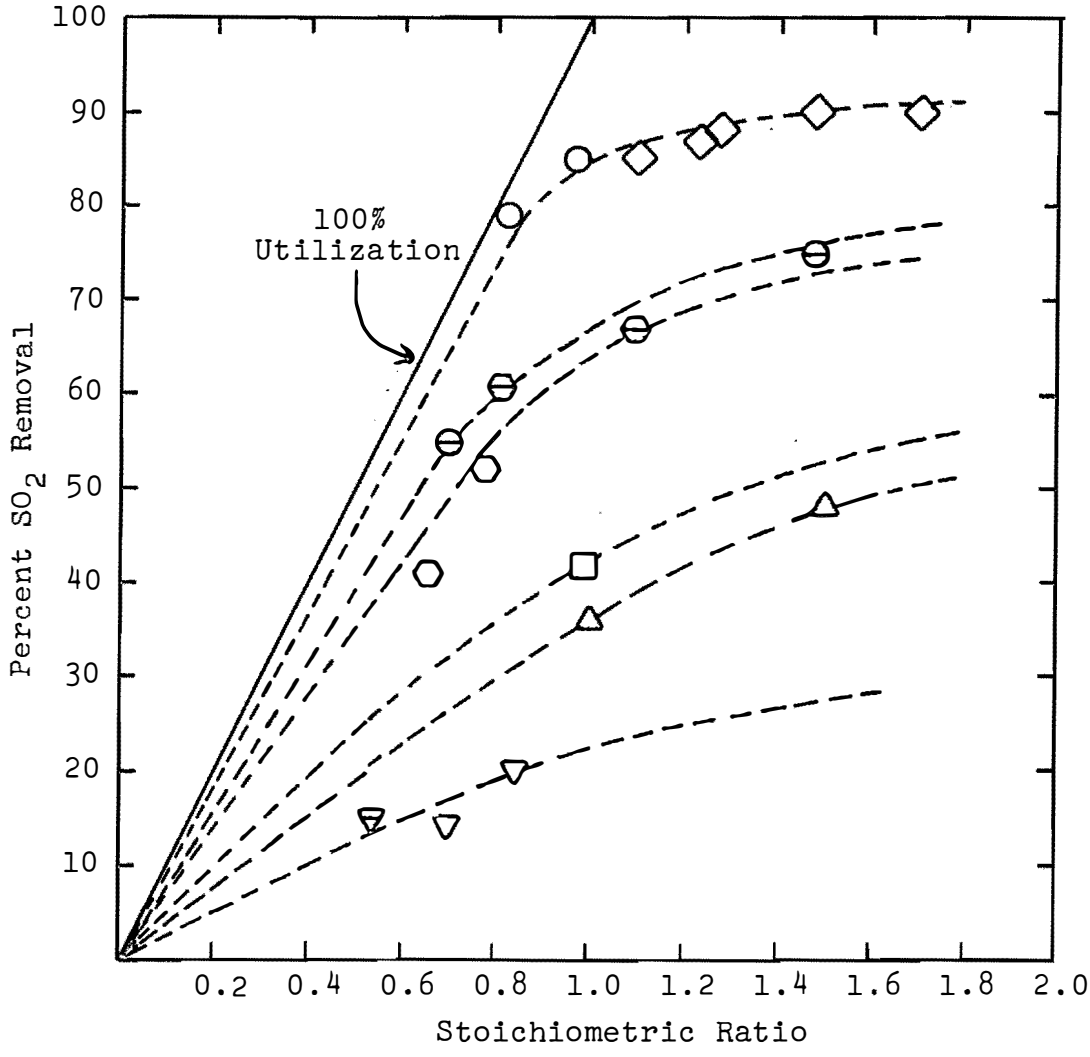

○	MMD=32 μm	B.H. Temp=300°F
⊖	MMD=32 μm	B.H. Temp=250°F
◇	MMD=32 μm	(1978 data) B.H. Temp=350°F
⬡	MMD=52 μm	B.H. Temp=300°F
⊖	MMD=52 μm	B.H. Temp=250°F
□	MMD=119 μm	B.H. Temp=300°F
△	MMD=154 μm	B.H. Temp=300°F
▽	MMD=193 μm	B.H. Temp=300°F
▽	MMD=193 μm	B.H. Temp=250°F

Figure 11. SO_2 Removal as a Function of $NaHCO_3$ Stoichiometric Ratio.

with the same system, were included. This was done to more completely illustrate the relationship between SO_2 removal and additive stoichiometric ratio.] Although the curves that appear in this figure are not valid outside the range of stoichiometry that each describes, the trend of the curves is apparent. At increasing stoichiometric ratios, the slopes of all the curves decrease. In fact, SO_2 removal efficiencies appear to "level out" at stoichiometric rates not much greater than 1.0.

Figure 11 was plotted without regard to the removal of additive by the bag house hopper. Five new data points were produced by disregarding the SO_2 removal and the stoichiometric contribution of that fraction of additive removed in the hopper. It was assumed that the desulfurization product was the same in both the hopper and filter cake samples. The sulfur concentration in the hopper and filter cake samples and the hopper collection efficiencies were used to modify the SO_2 removal and stoichiometric ratios of five tests. A detailed description of the calculation technique and a table of the "corrected" data points appear in Appendices D and E, respectively. The curves from Figure 11 were reproduced in Figure 12 along with the "corrected" data points. As illustrated in this figure, the SO_2 removal and stoichiometric ratio values obtained by compensating for hopper fallout were reasonably close to the curves that

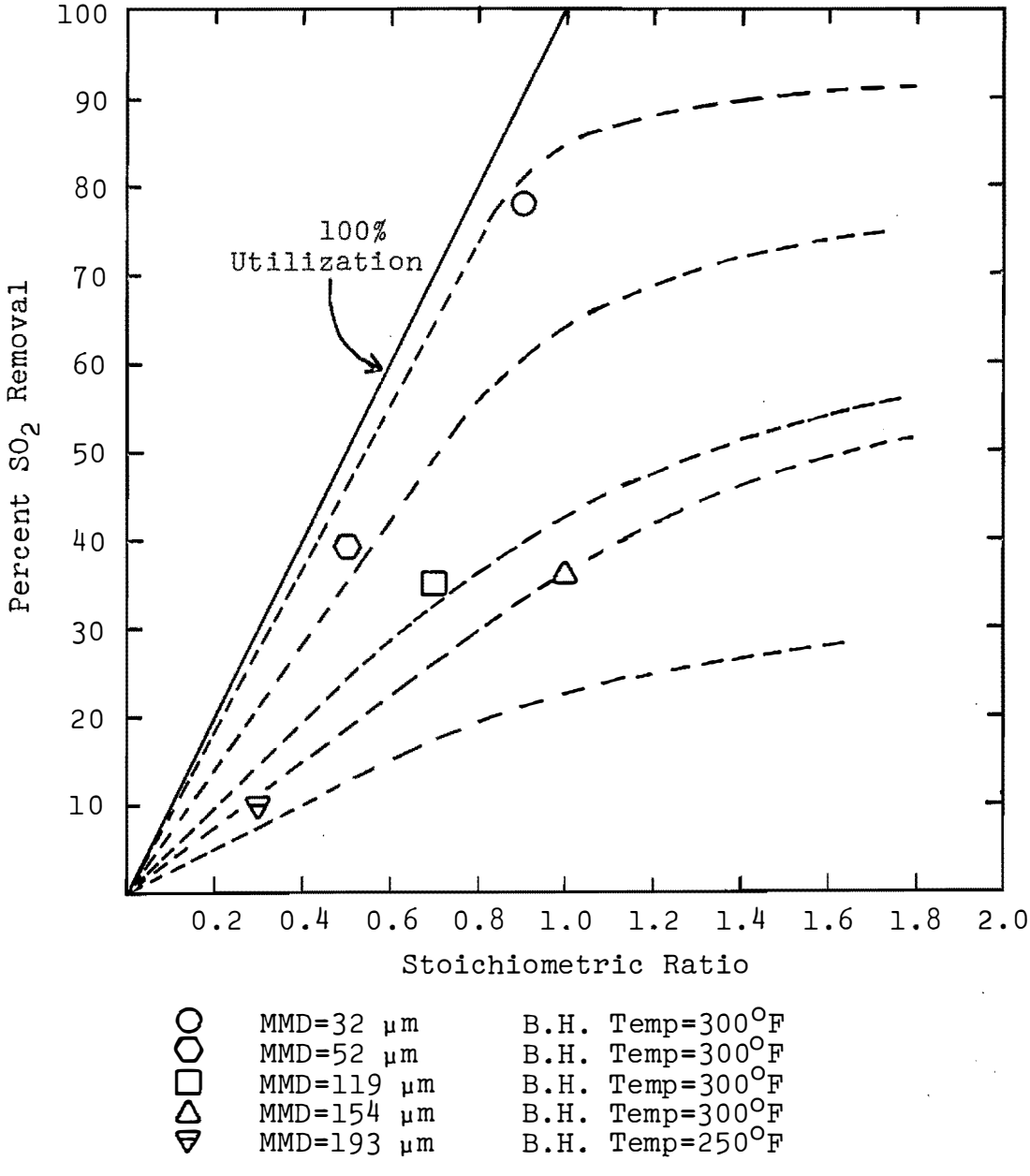

Figure 12. SO_2 Removal as a Function of $NaHCO_3$ Stoichiometric Ratio--Data Recalculated to Exclude Hopper Contribution.

were produced from the "uncorrected" values. No further attempt was made to correct either the SO_2 removal efficiency or the stoichiometric ratio to account for hopper fallout effects.

The additive mass mean diameter has a pronounced effect on SO_2 removal. This is evident from Figure 11. At a stoichiometric ratio of approximately 0.8 and a bag house temperature of approximately 300 degrees F, the following SO_2 removal efficiencies were observed: 20 % with MMD = 193μm, 52% with MMD = 52μm, and 79% with MMD = 32μm. At this temperature (bag house = 300 degrees F) increased removal was realized with injection of smaller $NaHCO_3$ dusts at all tested stoichiometric ratios. The effect of size was slightly different in the series of tests conducted at a bag house temperature of approximately 250 degrees F. SO_2 removal was greater with the injection of the MMD = 52 and MMD = 32μm powders than with the injection of the 193μm powder (see Figure 11). However, no appreciable difference was observed in the SO_2 removal results obtained with the smaller $NaHCO_3$ dusts (MMD = 32 and 52μm) at the lower temperature.

The effect of system temperature can also be discerned from Figure 11. Decreasing the bag house temperature from 300 to 250 degrees F did not produce any consequential change in the removal capabilities of the MMD = 193μm and MMD = 52μm $NaHCO_3$ additives. The effect

was, however, very different with the smallest additive (MMD = 32μm). At a bag house temperature of 300 degrees F and a stoichiometric ratio of 0.97, 85% of the SO_2 was removed at steady state conditions. With a reduction in bag house temperature to 250 degrees F the SO_2 removal was 75%, even though the additive feed rate was much higher (stoichiometric ratio of approximately 1.5). The results indicated that this effect occurs over the range of stoichiometric ratios tested (0.5-1.5).

Figure 13 illustrates how the SO_2 removal increased as a function of time with constant additive injection. The irregularities in the data are caused by fluctuations in the inlet, and consequently outlet, SO_2 conentrations. The steady state stoichiometric ratios have been calculated and are included in the figure. The rate of SO_2 removal increases most rapidly in the period just after additive injection is initiated. This corresponds physically to the period in which the filter cake is beginning to form on the bag surface. The rate of SO_2 removal increases more slowly as the filter cake develops, and finally approaches a steady state value.

The concept of the rate controlling step, as it applies to gas/solid reactions, can be applied to the $SO_2/NaHCO_3$ data obtained in this experiment. Whether the rate of mass transfer or the rate of chemical reaction

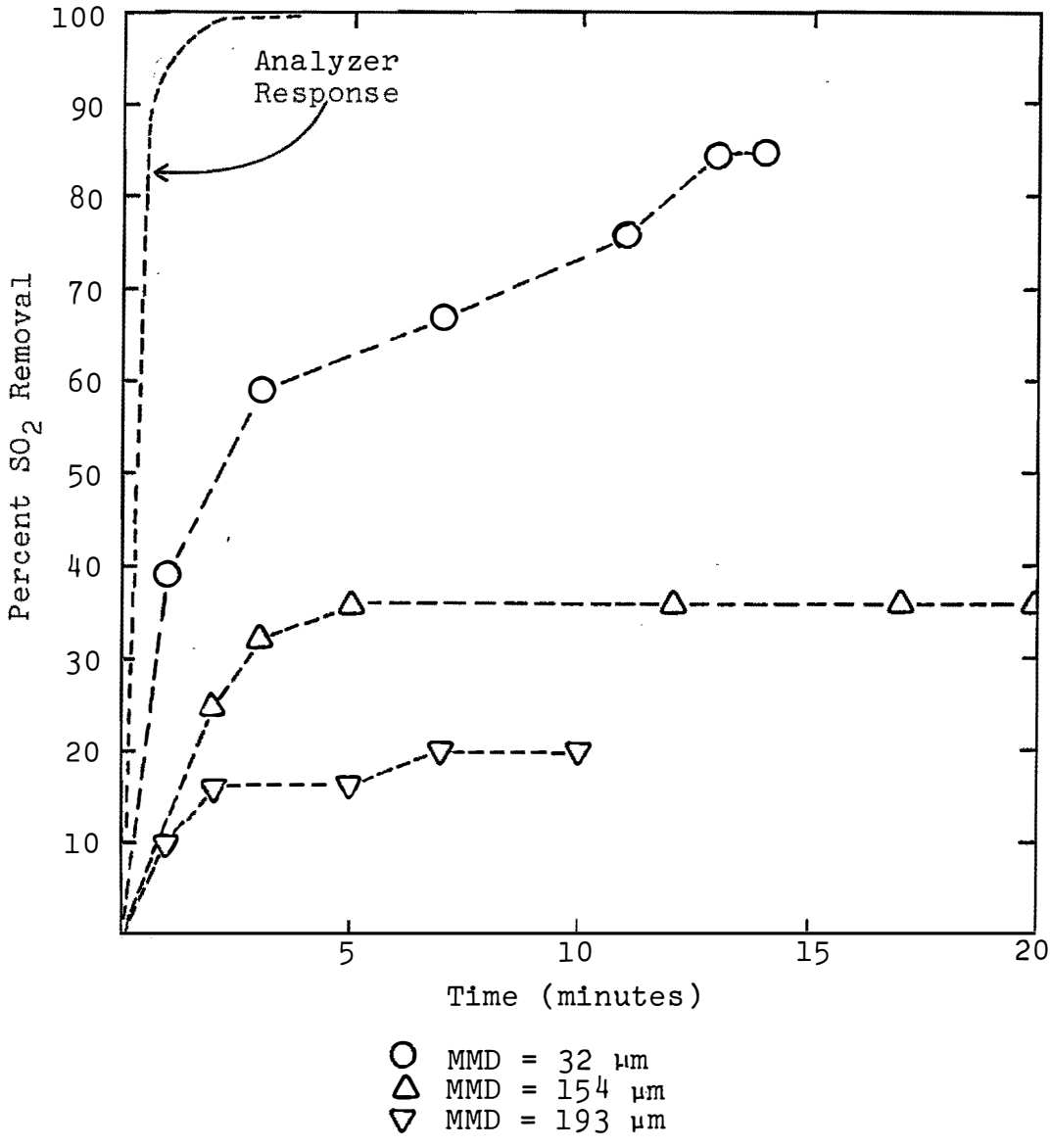

Figure 13. SO_2 Removal by $NaHCO_3$ as a Function of Time (B.H. Temp=300°F).

limits the overall removal of SO_2 depends on additive size. This is illustrated in Figure 8, p. 38.

The rate of mass transfer probably controls the overall rate of SO_2 conversion by the $NaHCO_3$ powders with mass mean diameters > 50μm. This is indicated by the combination of overall SO_2 removal sensitivity to particle size and insensitivity to decreased system temperature. Thus, assuming that the $SO_2/NaHCO_3$ reaction takes place as described by the unreacted-core model, either the rate of SO_2 diffusion through the boundary film (Figure 5, p. 31) or through the ash layer (Figure 6, p. 33) limits the overall reaction rate. Since the gas velocity was maintained at a constant value during the testing, it is not evident from the data whether one of these mass transfer steps is primarily responsible for the overall rate control at additive sizes > 50μm. However, it appears from the literature (7, 10, 11, 13) that ash layer resistance probably predominates over film resistance in reactions of this type.

Two chemical processes occur when $NaHCO_3$ is injected into a flue gas stream -- the decomposition of $NaHCO_3$ and the actual chemisorption of SO_2. Both are adversely effected by diminishing temperatures. One or both of these processes probably limits the overall rate of desulfurization by $NaHCO_3$ powders with mass mean diameters < 35μm. This is indicated by the decrease in

SO_2 removal that accompanied a decrease in system temperature. If the SO_2 and $NaHCO_3$ react as described in Equation 2 (without additive decomposition), the decrease in SO_2 removal can be attributed to a reduction in the chemical reaction rate. If, however, the SO_2 reacts with the decomposed additive (Na_2CO_3), Equations 1 and 3 must occur in series. Thus in this latter case, either the decomposition rate or the chemical reaction step may be limiting.

SO_2 Removal by Na_2CO_3

Seven separate tests were performed to evaluate the effect of particle size and system temperature on SO_2 removal by Na_2CO_3. The mass mean diameters of the samples fell roughly into the same size ranges as did the $NaHCO_3$ powders (see Table 3, p. 44). As with the $NaHCO_3$ testing, two temperature regimes were utilized, represented by bag house temperatures of 250 or 300 degrees F. The additive was fed at stoichiometric ratios from 0.7 to 2.0. The results and specific test conditions are tabulated in Appendix E.

A graphical representation of the SO_2 removal as a function of stoichiometric ratio appears in Figure 14. The SO_2 removal was generally poor. In fact, only the two smaller dusts (MMD = 27 and 42μm) were able to affect removal efficiencies > 10% at the conditions tested. Considering these two dusts, it was observed that

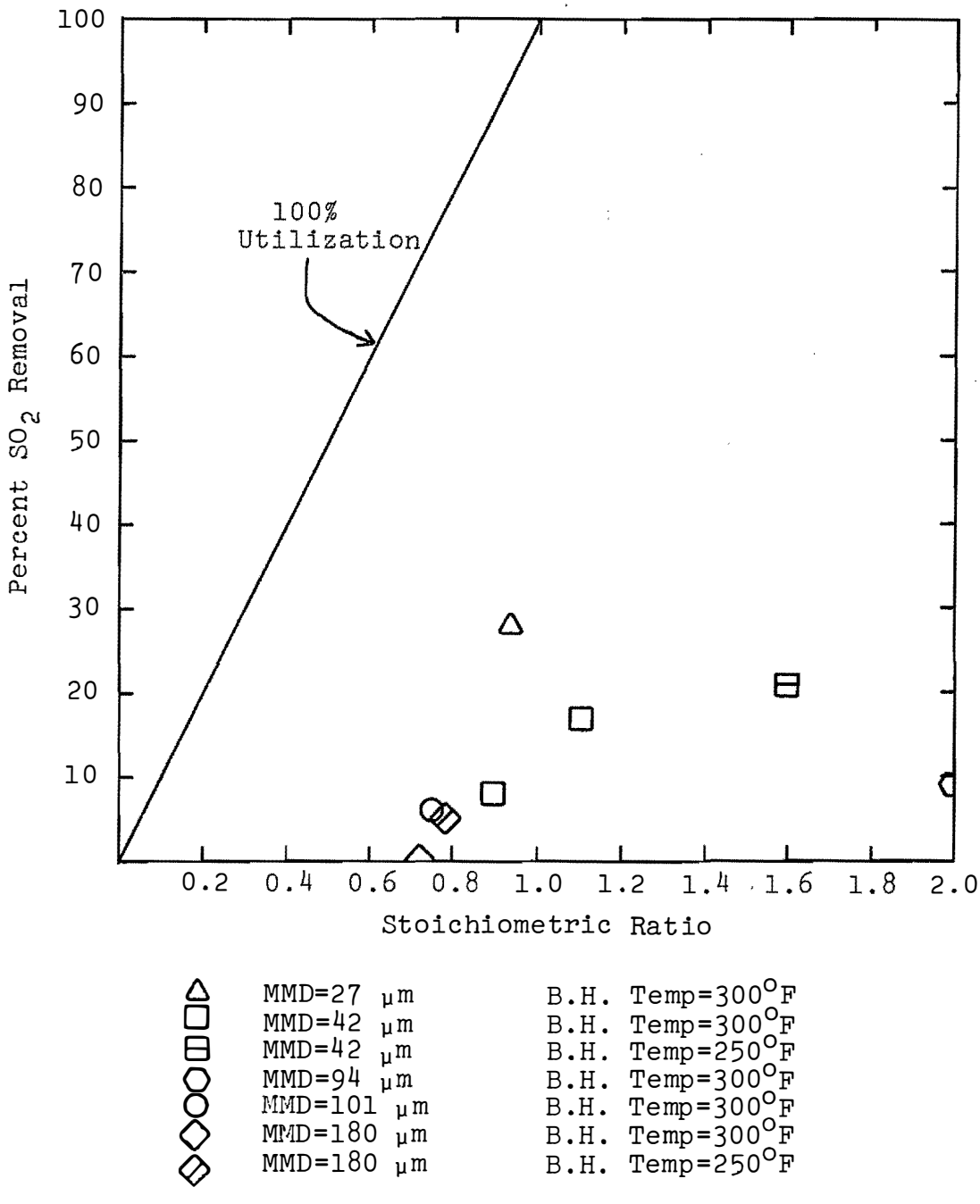

Figure 14. SO_2 Removal as a Function of Na_2CO_3 Stoichiometric Ratio.

decreasing the particle size appeared to increase the desulfurization efficiency. For example, at a bag house temperature of 300 degrees F and a stoichiometric ratio of about 0.9, the MMD = 27μm additive reduced the steady state concenration by 28% -- the corresponding reduction of the MMD = 42μm additive was 8%.

Two tests were conducted at a bag house temperature of 250 degrees F. No discernible effect on SO_2 removal was observed, although the data set was too small to allow specific generalizations.

The SO_2 removal capabilities of commercial and decomposed sodium bicarbonate can be demonstrated by comparing Figures 11 and 14. $NaHCO_3$ was found to be superior to Na_2CO_3 as a desulfurization additive. The maximum SO_2 removal attained with Na_2CO_3 injection was 28%; this occurred at a bag house temperature of 300 degrees F, a stoichiometric ratio of 0.94, and additive mass mean diameter of 27μm. Injection of $NaHCO_3$ additive of similar size (mass mean diameter of 32μm) into the system at a stoichiometric ratio of 0.82 at a bag house temperature of 300 degrees F yielded a SO_2 removal of 79%. Moreover, all sizes of $NaHCO_3$, with the exception of the largest (MMD = 193μm), affected greater SO_2 removal at all temperatures and stoichiometric ratios than the MMD = 27μm Na_2CO_3.

It has been widely assumed that the desulfurization of the flue gas by nahcolite ($NaHCO_3$) includes the intermediate step of $NaHCO_3$ decomposition to Na_2CO_3. The main reason for this assumption is that the Na_2CO_3 particle produced is much more porous than the parent material, consequently, better suited as a gas sorbent. It has been shown by this research effort that decomposition of $NaHCO_3$ in bulk prior to its addition to the flue gas stream had a detrimental effect on the resultant SO_2 removal efficiency. This can possibly be explained by one or more of the following postulations: firstly, SO_2 may react preferentially with pure $NaHCO_3$ at a faster rate than the decomposition of $NaHCO_3$ to Na_2CO_3; secondly, the method of decomposing the $NaHCO_3$ to Na_2CO_3 (heating in bulk) may have produced a less porous particle than that produced by injecting the $NaHCO_3$ directly into a rapidly moving gas stream; and thirdly, the optimum desulfurization reaction sequence may require that the SO_2 be present immediately after the pore forming process (liberation of CO_2 and H_2O). It could not be determined from the data acquired during this research effort which, if any, of the above postulations was responsible for the different performances of the additives.

NO Removal by $NaHCO_3$ and Na_2CO_3

The simultaneous removal of NO and SO_2 by the two sodium additives was measured in seventeen tests; some NO was removed in seven of them. Na_2CO_3 affected the removal of NO in only one of the seven tests in which that additive was injected. $NaHCO_3$ exhibited a larger capacity for NO sorption at the temperatures tested, since some NO was removed in six of the nine tests with that additive. By assuming that Equation 6 described the NO removal reaction, an additive/NO stoichiometric ratio (or Na/NO equivalent ratio) was calculated using the molar flow rates of NO and that portion of the additive that did not react with the SO_2. These values were computed and included in Appendix E. NO removal as a function of the Na/NO equivalent ratio is plotted in Figure 15. A maximum removal of 36% was obtained with injection of the MMD = 52μm $NaHCO_3$. It appeared that NO removal was not strongly dependent on additive size, since the maximum removal attained with the smallest $NaHCO_3$ powder (MMD = 32μm) was less than that of the MMD = 52μm powder -- 30% and 36% respectively. NO removal was also not dependent on the Na/NO equivalent ratio (see Figure 15).

The removal of NO does appear to be dependent on the system temperature. This is illustrated in Figure 16, in which increased temperature inhibits NO removal. For example, NO removal by the MMD = 52μm $NaHCO_3$ powder

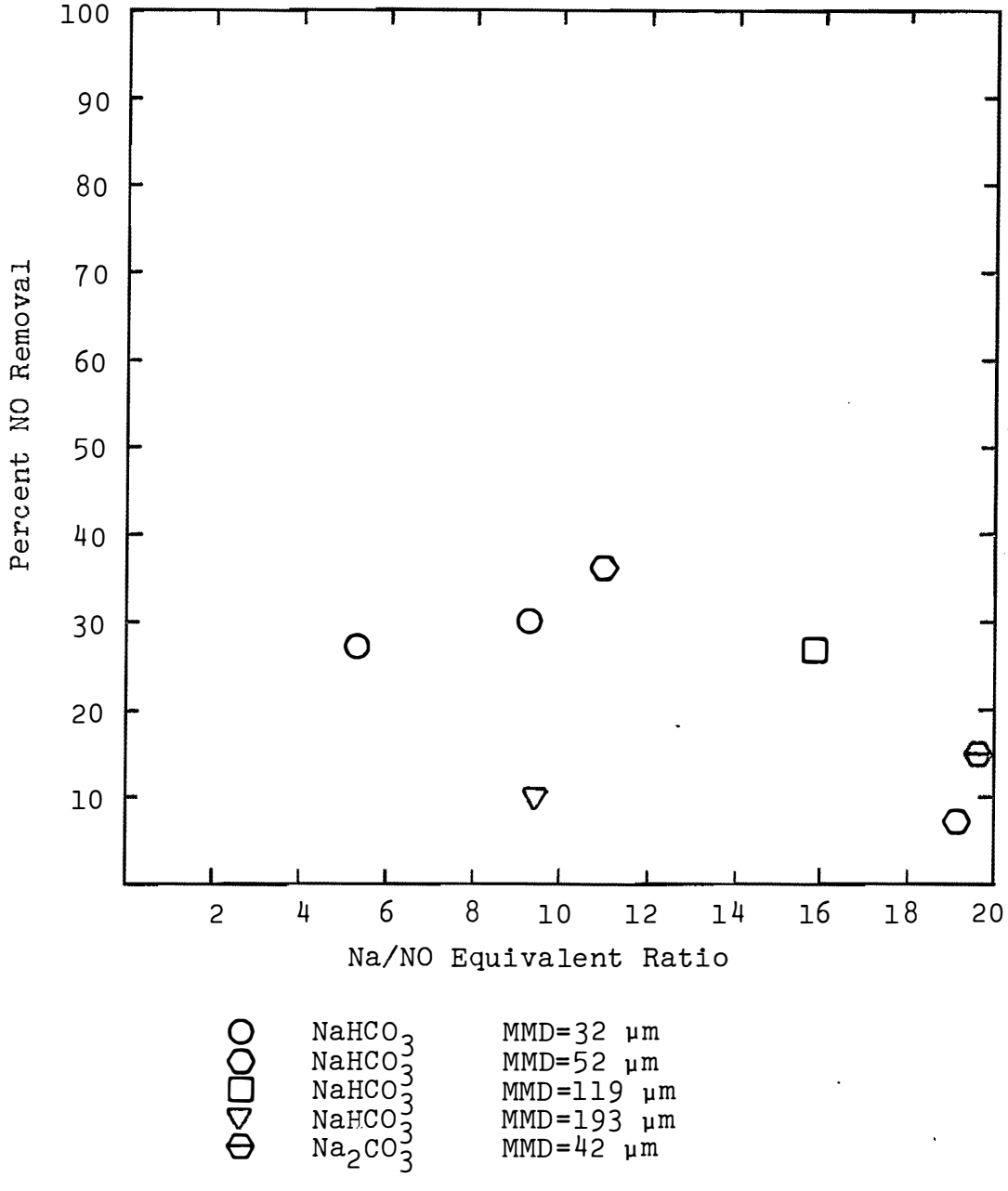

Figure 15. NO Removal as a Function of Na/NO Equivalent Ratio.

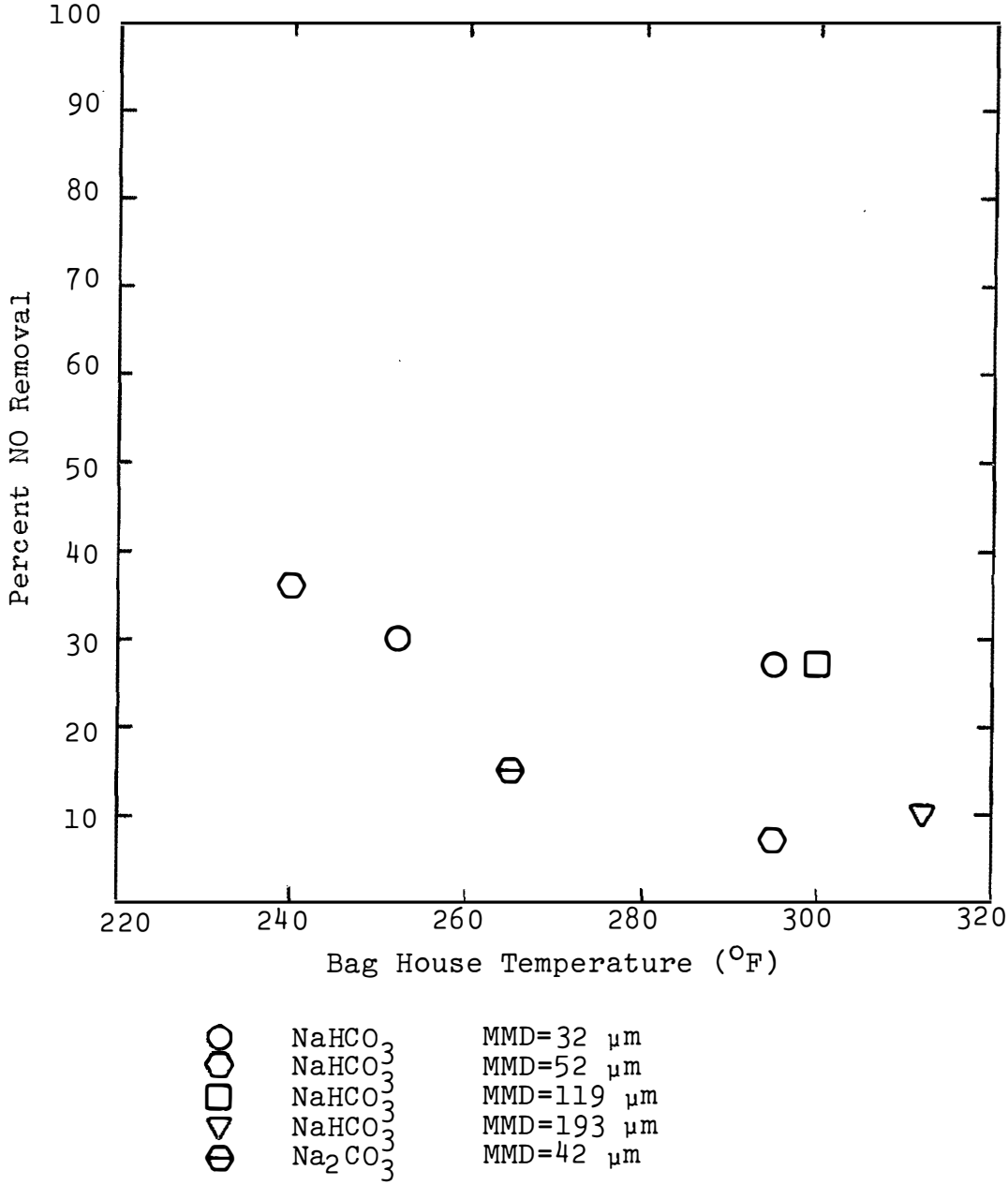

Figure 16. NO Removal as a Function of Bag House Temperature.

increased from 7% to 36% when the system temperature (represented by the bag house temperature) decreased from 295 to 240 degrees F.

V. CONCLUSIONS

The major conclusions arrived at as result of this investigation are summarized below.

1. It was demonstrated that 70% SO_2 removal (at steady state conditions) can be attained with two sizes of $NaHCO_3$ powders. In one case (additive MMD = 32μm, bag house temperature = 300 degrees F), a stoichiometric ratio of approximately 0.8 would be required. In the other case (additive MMD = 52μm, bag house temperature = 250 degrees F), a stoichiometric ratio of approximately 1.3 would be required.
2. Particle size, represented by mass mean diameter, has a greater effect on the desulfurization capacity of $NaHCO_3$ powders with MMD > 50μm than does varying the bag house temperature from 250 to 300 degrees F.
3. Decreasing the bag house temperature from 300 to 250 degrees F caused a reduction in the SO_2 removal capability of the smallest $NaHCO_3$ additive tested (MMD = 32μm).
4. When compared with the SO_2 removal capacity of pure $NaHCO_3$, decomposition of $NaHCO_3$ to Na_2CO_3 in bulk before injection yielded significantly poorer SO_2 removal.

5. In the tests in which the simultaneous removal of SO_2 and NO was measured, 7-36% of the NO was removed by the three smallest $NaHCO_3$ additives (MMD < 120μm).

6. No appreciable NO removal was observed with Na_2CO_3 injection.

7. Nitric oxide removal by $NaHCO_3$ was inversely dependent on the system temperature.

VI. RECOMMENDATIONS FOR ADDITIONAL RESEARCH

The following suggestions for additional research indicate areas in which the potentialities and limits of nahcolite (sodium bicarbonate) as a flue gas sorbent need to be established:

a. The optimum particle sizes for nahcolite (as well as other $NaHCO_3)/SO_2$ systems should be precisely defined.

b. The exact desulfurization reaction sequence should be determined at the molecular level.

c. Methods of $NaHCO_3$ decomposition other than the one employed herein (heating in bulk) should be investigated.

d. The optimum parameters for NO removal by nahcolite (and $NaHCO_3$) should be determined.

LIST OF REFERENCES

LIST OF REFERENCES

1. EPA. New Stationary Sources Performance Standards, Electric Utility Steam Generating Units, Federal Register 44, no. 113, June, 1979.

2. Liu, H. and R. Chaffee. Final Report on Evaluation of Fabric Filter as Chemical Contactor for Control of Sulfur Dioxide from Flue Gas, Contract PH22-68-51, Dept. of HEW, Public Health Service, NAPCA, Dec., 1969.

3. Veazie, F.M. and W.H. Kielmeyer. Feasibility of Fabric Filter as Gas - Solid Contactor to Control Gaseous Pollutants, Contract PH-22-68-64, Department of HEW, NAPCA, Aug., 1970.

4. Evaluation of Dry Alkalis for Removing Sulfur Dioxide from Boiler Flue Gases, EPRI Report FP-207, prepared by Bechtel Corp., Oct., 1976.

5. Hartman, M. "Comparison of Various Carbonates as Absorbents of Sulfur Dioxide from Combustion Gases," International Chemical Engineering, 18:712(1978).

6. Howatson, J., J. Ward Smith, D.A. Outka, and H.D. Dewald. "Nachcolite Properties Affecting Stack Gas Pollutant Absorption," Proceedings of 5th National Conference on Energy and the Environment, Cincinnati, Ohio, November, 1977.

7. Perry, R.H. and C.H. Chilton. Chemical Engineers' Handbook, 5th edition, New York: McGraw Hill, 1973.

8. Church and Dwight Sodium Bicarbonate (manufacturer's brochure), Church and Dwight Co., Inc., New York, N.Y.

9. Waters, P.L. "Fractional Thermogravimetric Analysis," Analytical Chemistry 32:852 (1960).

10. Knight, John H. The Use of Nahcolite for Removal of Sulfur Dioxide and Nitrogen Oxides from Flue Gas, The Superior Oil Co., 1977.

11. Stern, Frederic R. Bench-Scale Study of Sulfur and Nitrogen Oxides Adsorption by Nahcolite and Trona, Masters Thesis, University of North Dakota, 1978.

12. Genco, J.M. and H.S. Rosenberg. "Sorption of SO_2 on Ground Nahcolite Ore," JAPCA 26:989 (1976).

13. Levenspiel, O. Chemical Reaction Engineering, 2nd edition, New York: John Wiley and Sons, Inc., 1972.

14. Shah, N.D. and D.P. Teixeira. "Bench-Scale Evaluation of Dry Alkalis for Removing SO_2 from Boiler Flue Gases," presented at the Symposium on the Transfer and Utilization of Particulate Control Technology, Denver, Colo., 1978.

15. Ness, Harvey M. and Stanley J. Selle. Control of Western Power Plant Sulfur Dioxide Emissions: Development of the Ash-Alkali FGD Process and Dry Adsorption Techniques at the Grant Forks Energy Technology Center, Presented at the DOE Symposium on Environmental Control Activities, Washington, D.C., November, 1978.

16. Davis, W.T., T.C. Keener, and J.D. Leitman. "Research on the Removal of SO_2 by Additive Injection Techniques on a Stoker-Fired Boiler," 71st APCA Conference, Houston, Texas, June, 1978.

17. Davis, W.T., T.C. Keener, J.R. Carson, and H. Majdeski. "Study of SO_2 Removal in a Fabric Filter Collector by $NaHCO_3$ and Nahcolite Injection," submitted for publication to JAPCA, April, 1980.

18. Nahcolite Pilot Baghouse Study, Leland Olds Station, Stanton, North Dakota, Nonconfidential Test Data Section, 1977.

19. Szekely, J., J.W. Evans, and H.Y. Sohn. Gas-Solid Reactions, New York: Academic Press, 1976.

APPENDICES

APPENDIX A

SODIUM CARBONATE/SODIUM BICARBONATE ANALYSIS

1. A portion of the additive was dessicated for 24 hours. Approximately 1.0 gram of the sample was mixed with about 70 ml of distilled water and stirred for 5 minutes. The total sample volume was increased to 100 ml with distilled water. A 20 ml aliquot was then removed to a flask and titrated with 0.1 N HCL.

2. The aliquot from step 1 was titrated to the phenolphthalein end point. The percentage of Na_2CO_3 was calculated from the following equation:

$$\text{Percent } Na_2CO_3 = \frac{a(N)(\frac{1}{1000\ ml})(\frac{106\ g}{g\text{-}mole})\ x\ 100\%}{x\ (b/c)} \quad \text{(Eq. 10)}$$

where a = volume of HCl (ml)

b = volume of the aliquot before titration (ml)

c = total sample volume before titration (ml)

N = normality of the HCl solution $(\frac{g\text{-}mole}{l})$

x = grams of additive

3. The titration was then continued to the methyl orange end point. The percentage of $NaHCO_3$ was calculated from the following equation:

$$\text{Percent } NaHCO_3 = \frac{[a'-2a]N(\frac{1}{1000\ ml})(\frac{84\ g}{g\text{-}mole})\ x\ 100\%}{x\ (b/c)} \quad \text{(Eq. 11)}$$

where a' = total volume of HCl used (ml)

a = volume of HCl from step 2 (ml)

APPENDIX B

COULTER COUNTER® Model T&TA — **PARTICLE SIZE ANALYSIS**

.15 – 200μ
Σ PERCENT

COULTER ELECTRONICS INC.
590 W 20 ST.
HIALEAH, FLA. 33010

ORGANIZATION

OPERATOR JC 10-12-'79

EQUIPMENT

$k = d\sqrt[3]{2\pi}$ FOR MODEL T $\frac{A_2}{A_1} = \left(\frac{d_2}{d_1}\right)^3$ when $W_2 = W_1$ $\frac{A_2}{A_1} = \left(\frac{d_1}{d_2}\right)^3$ when $W_2 \neq W_1$ FOR MODEL TA

SAMPLE	ELECTROLYTE	DISPERSANT
#5-PF Bicarbonate	Non-aqueous	Ultrasonic

APER. SIZE	SERIAL		PART DIA.	W	± IA	A	SAMPLE SETTINGS DIA.	W	± IA	A
200										

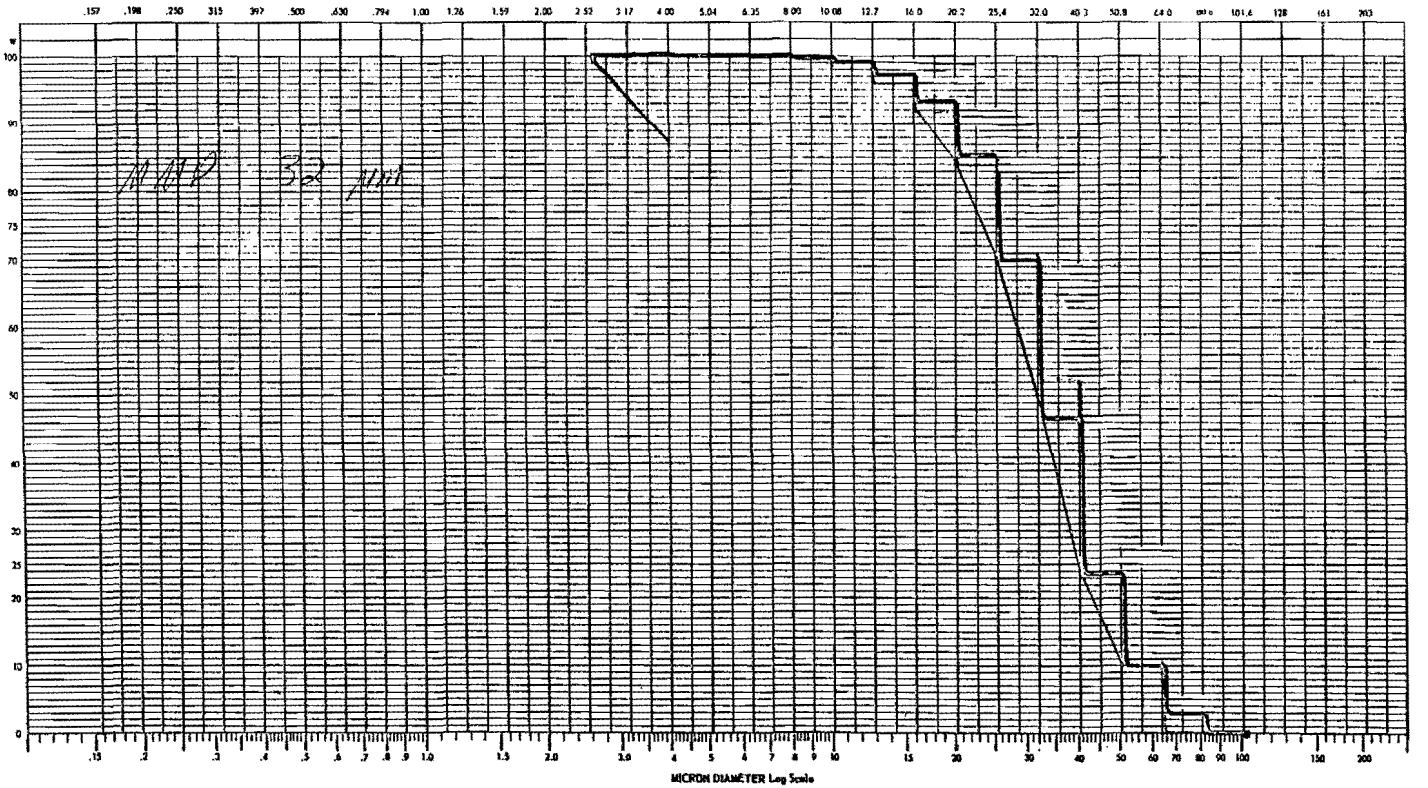

4221010

COULTER COUNTER® Model T&TA — **PARTICLE SIZE ANALYSIS**

.15 – 200 μ
X PERCENT

COULTER ELECTRONICS INC.
590 W 20 ST.
HIALEAH, FLA. 33010

ORGANIZATION

OPERATOR JC 9-28-'79

EQUIPMENT

$k = d\sqrt[3]{2^w}$ FOR MODEL T — $\frac{A_2}{A_1} = \left(\frac{d_2}{d_1}\right)^3$ when $W_2 = W_1$ — $\frac{A_2}{A_1} = \left(\frac{d_1}{d_2}\right)^3$ when $W_2 = W_1$ FOR MODEL TA

SAMPLE	ELECTROLYTE	DISPERSANT	APER. SIZE	SERIAL		PART DIA.	W	± TA	A	SAMPLE SETTINGS DIA.	W	± TA	A
A 3-DF	Non-aqueous	[illegible]	[illegible]										
Soda ash		[illegible]											

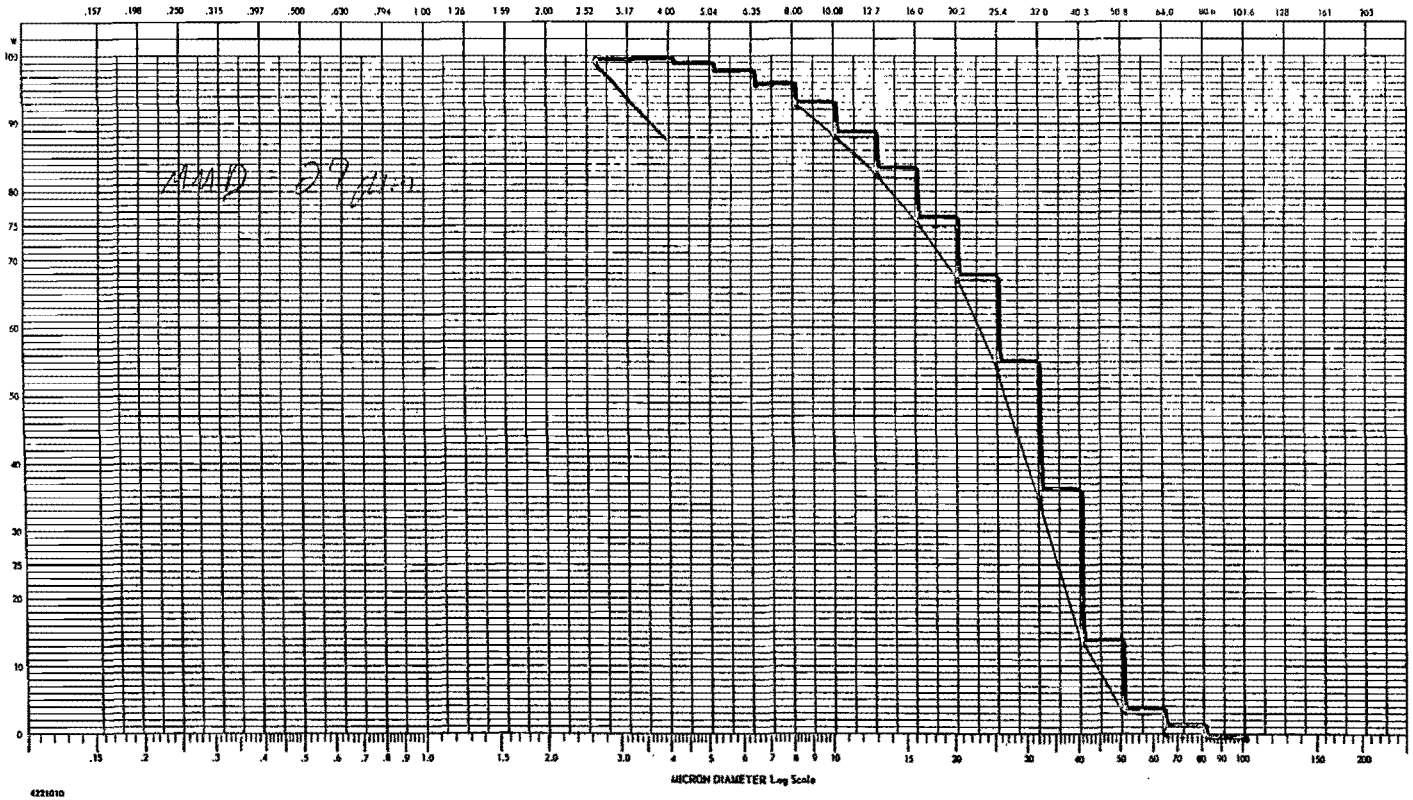

4221010

COULTER COUNTER® Model T&TA — **PARTICLE SIZE ANALYSIS**

.15 – 200 μ X PERCENT

COULTER ELECTRONICS INC.
590 W 20 ST.
HIALEAH, FL.A. 33010

ORGANIZATION

OPERATOR: JC – 10-12-79

EQUIPMENT

SAMPLE	ELECTROLYTE	DISPERSANT
#1 Bicarbonate	non aqueous	ultrasonic

$h = d\sqrt[3]{2w}$ FOR MODEL T; $\frac{A_2}{A_1} = \left(\frac{d_2}{d_1}\right)^3$ when $W_2 = W_1$; $\frac{A_2}{A_1} = \left(\frac{d_1}{d_2}\right)^3$ when $W_2 = W_1$ FOR MODEL TA

APER. SIZE	SERIAL		PART DIA.	W	± IA	A	SAMPLE SETTINGS DIA.	W	± IA	A
200										

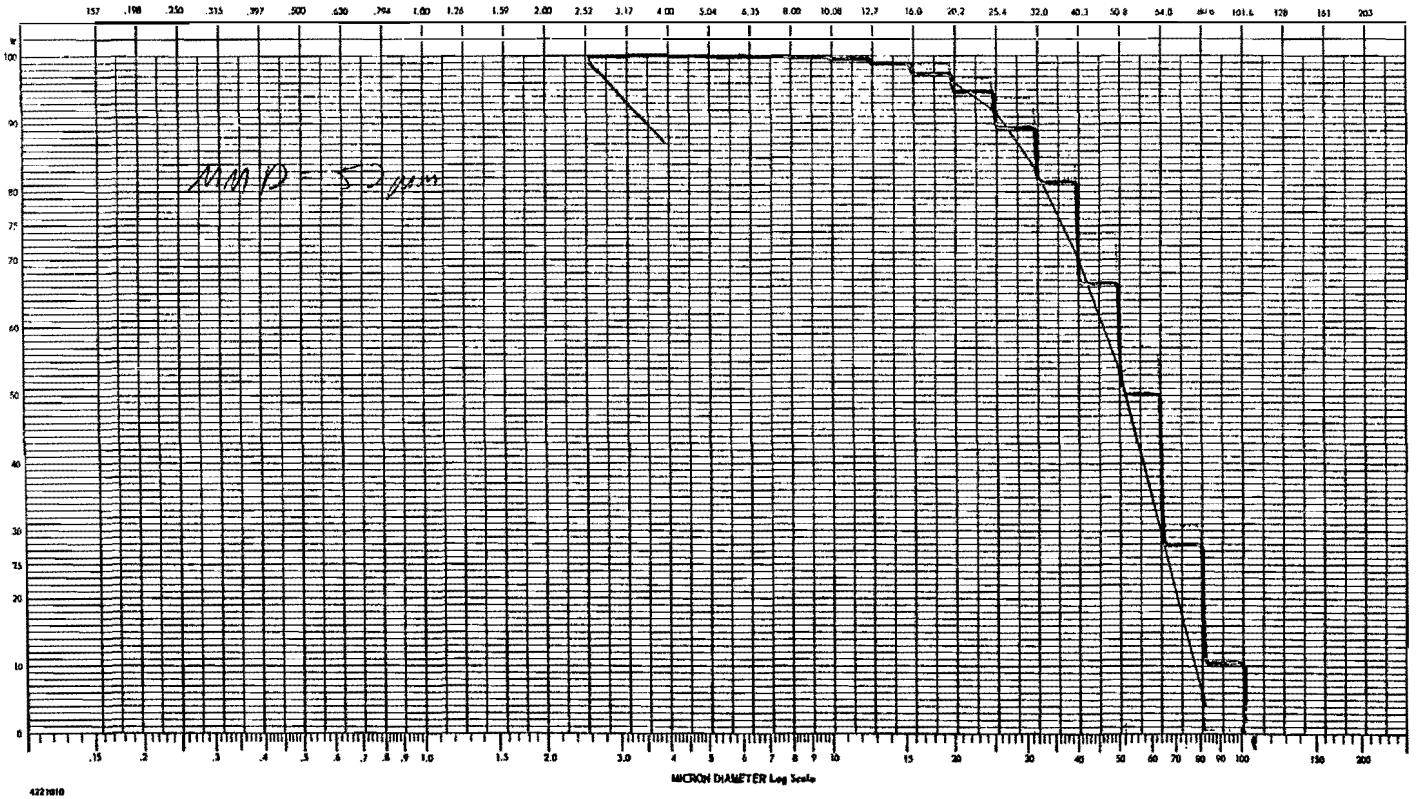

4221010

COULTER COUNTER® Model T & TA — **PARTICLE SIZE ANALYSIS**

.15 – 200μ
X PERCENT

COULTER ELECTRONICS INC.
590 W 20 ST.
HIALEAH, FLA. 33010

ORGANIZATION

OPERATOR JC

EQUIPMENT

$h = d\sqrt[3]{2^n}$ FOR MODEL T

$\frac{A_2}{A_1} = \left(\frac{d_1}{d_2}\right)^2$ when $W_2 = W_1$ FOR MODEL TA

$\frac{A_2}{A_1} = \left(\frac{d_1}{d_2}\right)^3$ when $W_2 = W_1$

SAMPLE	ELECTROLYTE	DISPERSANT
#2 Soda ash	Non-Aqueous	Ultrasonic

APER. SIZE	SERIAL	PART DIA.	W	± 1A	A	SAMPLE SETTINGS DIA.	W	± 1A	A

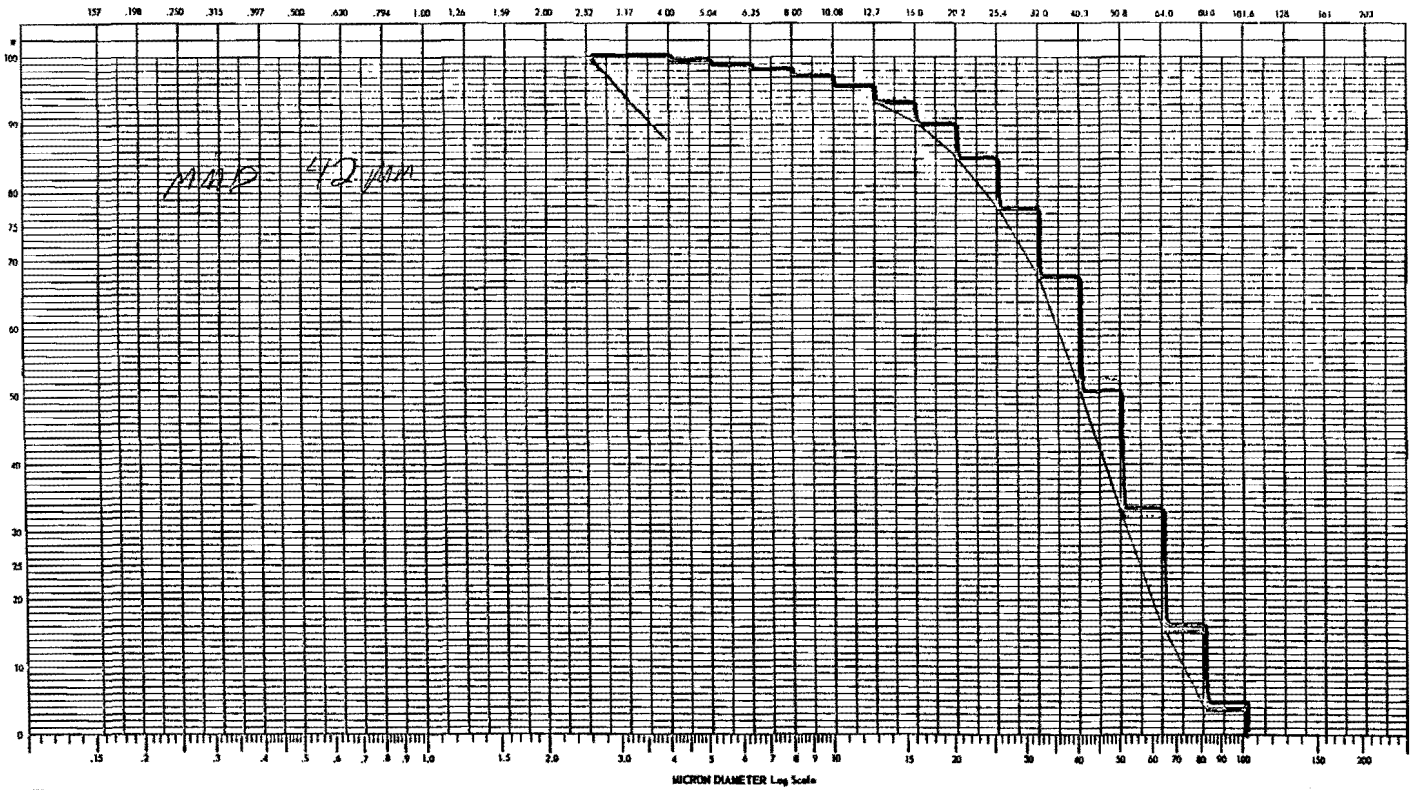

4221010

Table 4. Sieve Analysis of Additives

Additive	Cumulative Percent Passing Sieve 200-mesh	100-mesh	50-mesh	Mass Mean Diameter*
Bicarbonate #3DF	97.5	99.9		
Bicarbonate #1	60.7	98.7	100	67 μm
Bicarbonate #2	13.8	69.7	99.9	119 μm
Bicarbonate #4	5.7	44.1	99.9	154 μm
Bicarbonate #5	0.3	3.9	99.9	193 μm
Soda Ash #3DF	98.5	100		
Soda Ash #1	57.7	99.0	99.8	69 μm
Soda Ash #2	21.6	94.1	99.9	94 μm
Soda Ash #4	8.7	96.5	100	101 μm
Soda Ash #5	2.9	14.2	99.9	180 μm

*Estimated from log probability plots

APPENDIX C

TEST APPARATUS

1. Vibrascrew Feeder--Additive was injected with a vibrating, rotating screw-type conveyer. Additive rate control was affected by varying the rate of auger rotation.

2. Lear Siegler SM800 SO_2/NO Analyzer--NO was monitored at the system outlet for some tests. The analyzer measures the absorption of ultraviolet light by SO_2 and NO molecules.

3. Dynasciences CS-1000 SO_2 Analyzer--The inlet and outlet SO_2 concentrations were measured with this instrument. The analyzer measures the electrode potential change caused by the diffusion of SO_2 across a membrane.

4. Heated Sample Lines--Insulated, heated Teflon sampling lines that maintained the gas temperature above the dewpoint were employed to transport the sampled gas to the Dynasciences SO_2 analyzer.

5. Bacharach Fyrite Analyzers--Two analyzers were used to measure the volumetric O_2 and CO_2 content of the flue gas.

6. Fisher U.S. Signal Corps Mercury Barometer--This barometer was used to determine the local barometric pressure.

7. Fisher 470 Sulfur Analyzer--This analyzer was used to determine the weight percent sulfur in the ash samples. The analyzer utilizes an amperometric titration technique.

8. Coulter Counter Model TaII--The Coulter Counter was used to determine the size distributions of the smaller additives. A suspension of sample in an electrolyte is passed through a charged aperture. Since the pulse heights that result from this process are porportional to the particle volumes, the analyzer is able to produce a size distribution after enumerating the pulse heights.

9. Ro-Tap Tyler Sieve Shaker--The size distributions of the larger additives were determined by five minutes of shaking in this device. The sieve sizes utilized were 30, 50, 100, and 200-mesh.

APPENDIX D

CALCULATIONS

1. The percent moisture in the flue gas stream was determined from the following relationships:

$$\text{Percent moisture} = B_{ws} \times 100\% = \frac{P_w}{P_s} \times 100\% \qquad \text{(Eq. 12)}$$

where P_w = partial pressure of the water vapor in the flue gas stream (in. Hg)

P_s = absolute stack gas pressure (in. Hg)

Pw was obtained from the Carrier Equation.

$$P_w = P_{wB} - \frac{(P_s - P_{wB})(T_s - T_{wB})}{2830 - 1.44\ T_{wB}} \qquad \text{(Eq. 13)}$$

where P_{wB} = vapor pressure of water at the wet bulb temperature (in. Hg)

T_s = stack temperature (°F)

T_{wB} = stack wet-bulb temperature (°F)

2. The molar flow rate of SO_2 at the system inlet was determined from the following equation:

$$\dot{n}_{SO_2} = \hat{\rho}_{SO_2}\ Q_{std}\ C_{SO_2} \qquad \text{(Eq. 14)}$$

where $\dot{n}_{SO_2}$ = molar SO_2 flow rate $(\frac{\text{moles}}{\text{min}})$

$\hat{\rho}_{SO_2}$ = molar density of SO_2 at standard conditions (moles/ft^3)

Q_{std} = total volumetric flow rate at standard conditions (ft^3/min)

C_{SO_2} = fractional volumetric concentration of SO_2 in the gas stream

Thus, the actual molar flow rate of SO_2 through the system was determined by combining equations.

$$\dot{n}_{SO_2} = \hat{\rho}_{SO_2}\, C_{SO_2}\, Q_{act} \left(\frac{530°R}{T_s}\right)\left(\frac{P_s}{29.92 \text{ in. Hg}}\right)(1-B_{ws}) \qquad \text{(Eq. 15)}$$

where $\hat{\rho}_{SO_2} = 0.0027 \frac{\text{lb-moles}}{\text{ft}^3}$

Q_{act} = total volumetric flow rate at actual conditions = 963 ft^3/min.

3. The procedure for calculating the molar flow rate of NO at the system inlet was similar to that employed for the SO_2 flow rate calculation.

$$\dot{n}_{NO} = \hat{\rho}_{NO}\, Q_{std}\, C_{NO} \qquad \text{(Eq. 16)}$$

where $\dot{n}_{NO}$ = molar NO flow rate $\left(\frac{\text{lb-moles}}{\text{min}}\right)$

$\hat{\rho}_{NO}$ = molar density of NO at standard conditions = 0.0026 lb-moles/ft^3

Q_{std} = total volumetric flow rate at standard conditions (ft^3/min)

C_{NO} = fractional volumetric concentration of NO in the gas stream

4. The stoichiometric ratio was calculated for each test from the following equation:

$$S.R. = K \frac{\dot{n}_A}{\dot{n}_{SO_2}} \qquad \text{(Eq. 17)}$$

where $\dot{n}_A$ = additive molar flow rate $\left(\frac{\text{lb-moles}}{\text{min}}\right)$

$\dot{n}_{SO_2}$ = SO_2 molar flow rate $\left(\frac{\text{lb-moles}}{\text{min}}\right)$

K = stoichiometric coefficient

(K = 1/2 for $NaHCO_3$ additive; K = 1 for Na_2CO_3 additive)

5. The SO_2 removal was recalculated to disregard that

portion of the additive and sulfur product that were removed in the bag house hopper. It was assumed that the ultimate desulfurization product was the same in both the hopper and filter cake ash fractions. Firstly,

$$(\eta_{SO_2})_{bag} = \frac{S_{bag}}{S_{total}} (\eta_{SO_2})_{total} \qquad \text{(Eq. 18)}$$

where

$(\eta_{SO_2})_{bag}$ = SO_2 removal efficiency of that portion of the additive that was not collected in the hopper

$(\eta_{SO_2})_{total}$ = SO_2 removal efficiency by both the hopper and fabric ash fractions

S_{bag} = quantity of sulfur in that ash fraction collected on the fabric

S_{total} = the total quantity of sulfur in both the hopper and fabric ash fractions.

and

$$S = (M_{ash})Cs \qquad \text{(Eq. 19)}$$

where (M_{ash}) = mass of ash collected

Cs = concentration of sulfur per unit mass of ash

Combining Equations 18 and 19 yielded:

$$(\eta_{SO_2})_{bag} = \frac{(M_{ash})_{bag} (Cs)_{bag}}{(M_{ash})_{bag} (Cs)_{bag} + (M_{ash})_{hop} (Cs)_{hop}} \cdot (\eta_{SO_2})_{total} \qquad \text{(Eq. 20)}$$

The collection efficiency of the hopper on a mass basis (Ehop) could be estimated (see Figure 10). Since the sulfur concentration in the ash fractions (Cs) and the hopper collection efficiencies (Ehop) were known, an appropriate form of Equation 20 was used to estimate the SO_2 removal efficiency of the

additive that passed through the hopper and on to the bag surface.

$$(\eta_{SO_2})_{bag} = \frac{(100-Ehop)\ (Cs)_{bag}}{(100-Ehop)\ (Cs)_{bag} + Ehop\ (Cs)_{hop}}\ (\eta_{SO_2})_{total} \qquad \text{(Eq. 21)}$$

The SO_2 removal efficiency of that portion of the additive that was collected in the hopper was calculated with Equation 22.

$$(\eta_{SO_2})_{hop} = (\eta_{SO_2})_{total} - (\eta_{SO_2})_{bag} \qquad \text{(Eq. 22)}$$

6. The stoichiometric ratio that corresponds to a specific SO_2 removal efficiency obtained via Equation 21 can also be calculated. The appropriate stoichiometric ratios (from Equation 17) are

$$(S.R.)_{total} = \frac{K(\dot{n}_A)_{total}}{(\dot{n}_{SO_2})_{total}}$$

and $$(S.R.)_{bag} = \frac{K(\dot{n}_A)_{bag}}{(\dot{n}_{SO_2})_{bag}}$$

The additive molar flow rate, excluding that additive removed by the hopper, can be represented by the following equation:

$$(\dot{n}_A)_{bag} = (\dot{n}_A)_{total}\ \frac{(100-Ehop)}{100} \qquad \text{(Eq. 23)}$$

The SO_2 molar flow rate, excluding the SO_2 removed in the hopper fraction, can also be calculated.

$$(\dot{n}_{SO_2})_{bag} = (\dot{n}_{SO_2})_{total} \frac{[100-(\eta_{SO_2})_{hop}]}{100} \qquad \text{(Eq. 24)}$$

The stoichiometric ratio "corrected" to exclude the hopper contribution can be obtained by dividing Equation 23 by Equation 24 and multiplying by the stoichiometric coefficient.

$$(S.R.)_{bag} = \frac{(100-Ehop)(\dot{n}_A)_{total}\ K}{[100-(\eta_{SO_2})_{hop}]\ (\dot{n}_{SO_2})_{total}} \qquad \text{(Eq. 25)}$$

The form of Equation 25 that was actually used in the calculation procedure appears immediately below.

$$(S.R.)_{bag} = \frac{(100-Ehop)\ (S.R.)_{total}}{[100-(\eta_{SO_2})_{hop}} \qquad \text{(Eq. 26)}$$

APPENDIX E

Table 5. Test Data

Test #	Additive	B.H. Temp °F	Duct Temp °F	Percent Water Vapor	Percent O_2	Percent CO_2	SO_2 inlet (wet basis) ppm	SO_2 outlet (wet basis) ppm	Percent SO_2 Penetration	Percent SO_2 Efficiency	Additive/SO_2 Stoichiometric Ratio	NO inlet (wet basis)	NO outlet (wet basis)	Percent NO Penetration	Percent NO Efficiency	Na/NO Sodium Equivalent Ratio
1	1978 Bicarb #3DF	250	290	4.0	15.0	8.5	1200	290	24	76	2.30					
3	1978 Bicarb #30F	295	372	4.5	11.2	10.5	2820	820	29	71	1.35					
4	Bicarb #4	290	360	4.5	11.2	10.5	2800	1460	52	48	1.50	160	160	100	0	43.6
6	Soda #4	275	366	5.1	10.5	11.5	2560	2410	94	6	0.75	200	200	100	0	
7	Bicarb #4	312	388	5.1	10.5	11.5	1040	670	64	36	1.00	190	190	100	0	9.6
8a	Bicarb #5	312	388	5.1	10.5	11.5	1190	950	80	20	0.85	200	180	90	10	9.5
8b	Bicarb #5	312	388	5.1	10.5	11.5	1380	1190	86	14	0.70					
9	Bicarb #5	239	287	1.5	14.0	8.5	980	830	85	15	0.54	150	150	100	0	
10	Soda #5	245	294	1.5	14.0	8.5	1970	1870	95	5	0.78	130	130	100	0	
11	Soda #5	300	382	3.7	14.0	8.5	2170	2170	100	0	0.72	200	200	100	0	
12a	Soda #1	305	368	4.1	14.0	8.5	1730	1590	92	8	0.90	190	190	100	0	
12b	Soda #1	305	368	4.1	14.0	8.5	1440	1200	83	17	1.10					
13	Soda #2	300	364	5.8			1510	1370	91	9	2.00	230	230	100	0	
14a	Bicarb #1	295	354	5.8			2780	1640	59	41	0.66	140	130	93	7	19.2
14b	Bicarb #1	295	354	5.8			2360	1130	48	52	0.78					
15	Bicarb #2	300	364	5.8			2120	1230	58	42	0.99	220	160	73	27	15.9
17a	Bicarb #1	240	300	4.3	14.0	11.0	2250	880	39	61	0.81	220	140	64	36	11.0
17b	Bicarb #1	240	300	4.3	14.0	11.0	1720	570	33	67	1.10					
18	Soda #1	265	305	4.3	14.0	11.0	1340	1060	79	21	1.60	200	170	85	15	19.7
19a	Bicarb #3DF	252	306	6.6	14.5	8.0	1960	880	45	55	0.70	185	130	70	30	9.3
19b	Bicarb #3DF	252	302	6.6	14.5	8.0	930	230	25	75	1.48					
20a	Bicarb #3DF	295	372	5.9	16.0	7.0	1550	230	15	85	0.97	330	240	73	27	5.3
20b	Bicarb #3DF	295	372	5.9	16.0	7.0	1830	380	21	79	0.82					
21	Soda #3	325	412	5.9	16.0	7.0	1690	1220	72	28	0.94	340	340	100	0	

TABLE 6. Ash Analysis

Additive	Average Overall SO_2 Removal $(\eta SO_2)_{Total}$	Average Overall Stoichiometric Ratio $(S.R.)_{Total}$	Hopper Mass Efficiency (E_{Hop})	Percent Sulfur in Hopper Fraction $(C_s)_{Hop}$	Percent Sulfur in Fabric Fraction $(C_s)_{Bag}$	Baghouse Temperature ^oF	SO_2 Removal by Hopper Fraction $(\eta SO_2)_{Hop}$	SO_2 Removal by Fabric Fraction $(\eta SO_2)_{Bag}$	Stoichiometric Ratio Excluding Hopper Contribution $(S.R.)_{Bag}$
Bicarbonate (MMD=32μm)	82%	0.90	9%	6.38%	10.87	295°F	4%	78%	0.9
Bicarbonate (MMD=52μm)	47	0.72	30	5.60	11.27	295	8	39	0.5
Bicarbonate (MMD=119μm)	42	0.99	38	3.47	10.45	300	7	35	0.7
Bicarbonate (MMD=154μm)	48	1.50	45	5.92	11.75	290	14	34	1.0
Bicarbonate (MMD=193μm)	15	0.54	50	1.66	3.68	239	5	10	0.3
Soda Ash (MMD=42μm)	13	1.00	20	1.95	3.19	285	2	11	0.8

VITA

John Robert Carson was born in Knoxville, Tennessee on July 6, 1950. He attended public schools in Oneida, Tennessee and was graduated from Oneida High School in June 1968. He entered the University of Tennessee, Knoxville and received a Bachelor of Science degree in Education with a major in Biological Science in June 1973.

He was employed by White Lily Foods, Inc. through the summer of 1977. He entered the University of Tennessee in the fall of 1977 and received a Master of Science degree in Environmental Engineering in August 1980.

The author is a member of the Air Pollution Control Association.

He is married to the former Carolyn Newport of Oneida, Tennessee.